AD_____

Award Number: W81XWH-05-1-0390

TITLE: Chemoprevention of Breast Cancer by Mimicking the Protective Effect of Early First Birth

PRINCIPAL INVESTIGATOR: Malcolm C. Pike, Ph.D.

CONTRACTING ORGANIZATION: University of Southern California
Los Angeles, CA 90089-1147

REPORT DATE: June 2007

TYPE OF REPORT: Annual

PREPARED FOR: U.S. Army Medical Research and Materiel Command
Fort Detrick, Maryland 21702-5012

REPORT DOCUMENTATION PAGE

Form Approved
OMB No. 0704-0188

1. REPORT DATE *(DD-MM-YYYY)*	**2. REPORT TYPE**	**3. DATES COVERED** *(From - To)*
01-06-2007	Annual	2 May 2006 – 2 May 2007

4. TITLE AND SUBTITLE

Chemoprevention of Breast Cancer by Mimicking the Protective Effect of Early First Birth

5a. CONTRACT NUMBER

5b. GRANT NUMBER
W81XWH-05-1-0390

5c. PROGRAM ELEMENT NUMBER

6. AUTHOR(S)

Malcolm C. Pike, Ph.D.

E-Mail: mcpike@usc.edu

5d. PROJECT NUMBER

5e. TASK NUMBER

5f. WORK UNIT NUMBER

7. PERFORMING ORGANIZATION NAME(S) AND ADDRESS(ES)

University of Southern California
Los Angeles, CA 90089-1147

8. PERFORMING ORGANIZATION REPORT NUMBER

9. SPONSORING / MONITORING AGENCY NAME(S) AND ADDRESS(ES)
U.S. Army Medical Research and Materiel Command
Fort Detrick, Maryland 21702-5012

10. SPONSOR/MONITOR'S ACRONYM(S)

11. SPONSOR/MONITOR'S REPORT NUMBER(S)

12. DISTRIBUTION / AVAILABILITY STATEMENT
Approved for Public Release; Distribution Unlimited

13. SUPPLEMENTARY NOTES – Original contains colored plates: ALL DTIC reproductions will be in black and white.

14. ABSTRACT

We have successfully shown that in the rat estradiol, estradiol plus progesterone, and beta-HCG is protective against carcinogen-induced mammary tumorigenesis. Progesterone alone was not protective. Also, treatment with perphenazine was partially protective. We have continued to collect normal breast tissue from women undergoing elective reduction mammoplasty. Estrogen receptor and progesterone receptor have been characterized as well as cell proliferation have been characterized in these samples. Two chemoprevention protocols have been developed and are set to begin recruitment in the near future. The first will evaluate the role of high dose progestins on cell proliferation and gene expression profiles in the breast. The second protocol will evaluate the role of various oral contraceptive progestin doses on cell proliferation and gene expression profiles in the breast.

15. SUBJECT TERMS
No subject terms

16. SECURITY CLASSIFICATION OF:			**17. LIMITATION OF ABSTRACT**	**18. NUMBER OF PAGES**	**19a. NAME OF RESPONSIBLE PERSON**
a. REPORT	**b. ABSTRACT**	**c. THIS PAGE**			USAMRMC
U	U	U	UU	37	**19b. TELEPHONE NUMBER** *(include area code)*

Standard Form 298 (Rev. 8-98)
Prescribed by ANSI Std. Z39.18

Table of Contents

Page

INTRODUCTION: This Innovator Award is designed to provide insight into the ways in which a chemoprevention regimen can mimic the protective effect of a full-term pregnancy (a birth) against breast cancer. In addition, we are aiming to understand the mechanisms underlying the risk associated with increased mammographic density, the strongest known risk factor for breast cancer after the highly penetrant genetic risk factors of BRCA1 and BRCA2 mutations. Mammographic densities are permanently reduced by births; and this relationship is being explored in depth in order to determine if this is an important part of the mechanism by which births provide protection against breast cancer. This work is being conducted both in humans and rodents.

BODY: The Innovator Award consists of four projects (Projects 1 and 2 are being completed through a subcontract to our colleague Dr. Lewis Chodosh at the University of Pennsylvania, and Projects 3 and 4 are being completed by the team at USC).

Projects 1 and 2 involve both rat and human components and consists of 10 tasks.

Task 1: Months 1-12: Treat rats with different hormonal chemoprevention regimens, harvest mammary tissue, and isolate RNA.

This task has been completed on schedule. Groups of Lewis rats have been treated with pellets containing either estradiol, progesterone, estradiol and progesterone, beta-HCG, or perphenzine. Animals were treated for 21 days. Pellets were then removed and animals sacrificed 28 days later. Control groups consisted of parous animals allowed to undergo a single round of pregnancy, lactation, and 28 days of involution, as well as age-matched nulliparous controls. For all groups, total RNA was prepared from mammary glands by ultracentrifugation through a CsCl/guanidinium isothiocyanate cushion.

The effects of each of these hormonal treatments on the susceptibility to MNU-induced mammary tumorigenesis was tested using standard protocols either with MNU administered before hormonal treatments or after. Similar results were obtained and confirmed that treatment with estradiol, estradiol and progesterone, or beta-HCG is protective against mammary tumorigenesis, whereas treatment with progesterone is not. Additionally, we found that treatment with perphenazine was partially protective against MNU-induced tumorigenesis.

Task 2: Months 6-24: Analyze morphological changes and determine global gene expression profiles for rat mammary gland samples from rats treated with different hormonal chemoprevention regimens.

This task has been completed on schedule. Analysis of mammary gland morphology by carmine stained whole mounts as well as by hematoxylin and eosin-stained sections indicated that after 21 days of hormone treatment, estradiol, estradiol and progesterone, beta-HCG, and perphenazine each gave rise to mammary epithelial differentiation comparable to that observed in mid-pregnant animals. In contrast, treatment with

progesterone had no effect on mammary epithelial morphology.

Mammary gland morphology was also examined following 28 days of involution following treatment termination. This analysis revealed that mammary gland morphology was extremely similar among all groups and that there were not obvious differences in the amount of epithelium present.

RNA prepared from each of these experimental groups was used to generate biotinylated cRNA suitable for hybridization to Affymetrix oligonucleotide microarrays. Each of these samples was subsequently hybridized to Affymetrix microarrays. Array results have been analyzed and quality control parameters have confirmed successful hybridization and scanning of the arrays. Analyses of these microarray data sets have also been performed to identify genes that are differentially expressed as a consequence of each hormonal treatment regimen, and analyses are in progress to identify genes that are differentially expressed in response to protective, but not non-protective, hormonal treatments.

Task 3: Months 6-36: Identify genes that are expressed in a parity-specific manner in the rat.

This task has been completed ahead of schedule and was published in *Cancer Research* (Blakely et al., 66:6421-6431, 2006), where it was featured on the cover.

A major challenge posed by global gene expression surveys is the large number of differentially expressed genes that are typically identified, only a few of which may contribute causally to the phenomenon under study. Consequently, we considered approaches to identifying parity-induced changes in the rat mammary gland that would permit the resulting list of expressed genes to be narrowed to those most robustly associated with parity-induced protection against mammary tumorigenesis. Given the marked genetic and biological heterogeneity between different inbred rat strains, we reasoned that identifying expression changes that are conserved across multiple strains exhibiting hormone-induced protection against mammary tumorigenesis would facilitate the identification of a core set of genes associated with parity-induced protection against breast cancer.

To achieve this goal, we focused on gene expression changes that are conserved among different strains of rats that exhibit hormone-induced protection against mammary tumorigenesis. Four inbred rat strains that exhibit marked differences in their intrinsic susceptibilities to carcinogen-induced mammary tumorigenesis were each demonstrated to display significant protection against MNU-induced mammary tumorigenesis following treatment with pregnancy levels of estradiol and progesterone. Microarray expression profiling of parous and nulliparous mammary tissue from these four strains yielded a common 70-gene signature. Examination of the genes constituting this signature implicated alterations in TGF-beta signaling, the extracellular matrix, amphiregulin expression, and the growth hormone-Igf1 axis in pregnancy-induced alterations in breast cancer risk. Notably, related changes have been associated with decreased mammographic density, which itself is strongly associated with decreased breast cancer risk. Our findings demonstrate that hormone-induced protection against

mammary tumorigenesis is widely conserved among divergent rat strains and define a gene expression signature that is tightly correlated with reduced mammary tumor susceptibility as a consequence of a normal developmental event. Given the conservation of this signature, these pathways may contribute to pregnancy-induced protection against breast cancer.

Task 4: Months 6-36: Identify genes whose expression in rats correlates with protection against breast cancer.

This task has been completed ahead of schedule. To narrow the list of candidate genes whose regulation might contribute to the protected state associated with parity, we attempted to identify parity-induced gene expression changes that correlated with protection across multiple rat strains. To this end, total RNA was isolated from the mammary glands of nulliparous and parous Wistar-Furth, Fischer 344, and Copenhagen rats and analyzed on RGU34A arrays. This led to the identification of 68, 64 and 92 parity-up-regulated genes and 132, 209 and 149 parity-down-regulated genes in Wistar-Furth, Fischer 344, and Copenhagen rats, respectively.

Unsupervised hierarchical clustering performed using the expression profiles of 1,954 globally varying genes across the nulliparous and parous datasets representing the four rat strains revealed that samples clustered primarily based on strain without regard to parity status. This suggested that the principal source of global variation in gene expression across these data sets was due to genetic differences between strains rather to than reproductive history. This observation suggested that determining which parity-induced gene expression changes were conserved among these highly divergent rat strains could represent a powerful approach to defining a parity-related gene expression signature correlated with hormone-induced protection against mammary tumorigenesis.

To identify parity-induced gene expression changes that were conserved across strains, we selected genes that exhibited $\geq$ 1.2-fold change in at least of 3 of the 4 strains analyzed. This led to the identification of 24 up-regulated and 46 down-regulated genes. Based on the number of parity-induced gene expression changes observed for each strain, an overlap of this size is highly unlikely by chance (up-regulated: $P<1x10^{-6}$, FDR < 1%; down-regulated: $P<1x10^{-6}$, FDR = 4%). As such, this approach led to the identification of a set of genes whose expression is persistently altered by parity across multiple strains of rats that exhibit hormone-induced protection against mammary tumorigenesis.

To confirm the validity of the parity-related gene expression signature derived from the above studies, we performed oligonucleotide microarray analysis on samples from nulliparous and parous Lewis rats that were generated independently from those used to derive this signature. Hierarchical clustering analysis of these independent samples using the gene signature revealed that the expression profiles of these genes were sufficient to accurately distinguish parous from nulliparous Lewis rat samples in a blinded manner.

To determine whether this parity-related signature could distinguish between nulliparous and parous mammary glands from multiple strains of rats, Lewis, Wistar-Furth, Fischer 344, and Copenhagen microarray data sets were clustered in an

unsupervised manner based solely on the expression of the genes comprising the parity signature. In each of the four rat strains examined, the gene expression signature was sufficient to distinguish parous from nulliparous rats. Thus, this signature reflects parity-induced gene expression changes that are highly conserved among four genetically divergent rat strains.

Among the genes that we identified as being consistently regulated by parity, at least five categories were evident. These included the previously identified differentiation, immune, Tgf-beta, and growth factor categories, as well as an additional category of genes that are involved in extracellular matrix (ECM) structure and function. We next demonstrated that clustering based upon genes in each of these five categories was sufficient to distinguish between nulliparous and parous mammary samples from each of the four different rat strains, from independent mammary samples derived from nulliparous and parous Lewis rats, and from mammary samples derived from FVB mice. These findings indicate that differential expression of these five subsets of genes represent conserved features of parity-induced changes in the rodent mammary gland. Our findings have now been published in *Cancer Research* (Blakely et al., 66:6421-6431, 2006).

Task 5: Months 1-48: Isolate RNA from human mammary gland samples and control epithelial and stromal samples.

Per the SOW, significant progress has been made on this aim. RNA has been isolated from a large number of the available human specimens. In addition, we have prepared RNA from control samples consisting of: intact adipose tissue, intact fibrous (e.g. stromal and epithelial) breast tissue, epithelial organoids isolated by collagenase digestion, cultured epithelial organoids, and cultured fibroblasts from reduction mammoplasty specimens. Quality control analysis of isolated RNA indicates that some samples have suffered significant RNA degradation. The extent of degradation observed is variable, and appears to be determined primarily by the sample itself, rather than the procedure used, suggesting that the issue may be related to the manner in which the tissue was originally harvested.

Task 6: Months 3-52: Determine global gene expression profiles for human mammary gland samples using oligonucleotide microarrays.

Per the SOW, work on this aim has been initiated and progress has been made. Biotinylated cRNA has been prepared from a subset of the RNA samples isolated in Task 5 and proof-of-principle experiments have been performed to demonstrate that these samples can be run on Affymetrix microarrays and meet established quality control standards. Over the past study period, obtaining high-quality RNA without degradation has been prioritized over performing additional array hybridizations.

Task 7: Months 12-60: Identify genes whose expression in the mammary gland in women reflects aspects of reproductive history that impact on breast cancer susceptibility.

Per the SOW, this task was initiated in the previous study period. To date, the relatively small number of arrays that have been run, and the large number of reproductive variables that need to be analyzed, has precluded the identification of any genes. These will presumably emerge as these studies proceed over the next three study periods.

Task 8: Months 1-36: Determine the effect of short-term, low-dose estradiol and progesterone treatment on MNU-induced mammary tumor susceptibility.

Per the SOW, work on this aim has been initiated and continues to determine whether hormone-induced protection against carcinogen-induced tumors can be provided by lower dose or shorter term estradiol treatment than standard regimens that have been applied in the past.

Task 9: Months 12-60: Determine the effect of hormone treatment on MNU-induced mammary epithelial proliferation.

Per the SOW, this task was initiated in the last study period. Mammary epithelial proliferation rates will be assessed in the mammary glands of rats that have or have not previously been treated with estradiol and progesterone following acute treatment with MNU.

Task 10: Months 12-60: Determine whether p53 loss abrogates pregnancy-induced protection against carcinogen-induced mammary tumorigenesis.

As Tasks 3 and 4 above were completed one year ahead of schedule, the initiation of work on Task 10 was temporarily delayed to permit the completion of these other studies. This task will be initiated in the next study period.

Project 3

This project aims to recruit subjects being treated with a variety of hormonal regimens to have pre- and/or post-treatment breast biopsies. The treatment with the hormonal agents may or may not be a study procedure. A number of hormonal, genetic and cellular analyses will be carried out on the biopsy specimens obtained before and/or after the treatment regimen.

Task 1. Months 1-6: Develop an appropriate protocol and treatment regimen.

To date we have developed three protocols directly related to this statement of work and fourth protocol which has been funded through other mechanisms, but is critical in providing data relevant to the overall goals of this SOW.

The first protocol we developed involves obtaining pre- and and post-treatment biopsies for women receiving high dose progestins for the treatment of endometrial hyperplasia. This protocol is developed, has USC IRB approval and is pending approval of the revised SOW and the DOD IRB. We will recruit 10 women receiving high dose progestin (Megace) for the treatment of endometrial hyperplasia (as standard of care). For this research protocol, the subjects will receive a breast biopsy before Megace treatment, and after three months of Megace treatment. We will evaluate the effect of this progestin on genetic and cellular characteristics of the breast tissue.

The second protocol we developed involves obtaining breast biopsies from women randomized to two different doses of oral contraceptives. This protocol has been approved by the USC IRB with contingencies and will be submitted to the DOD IRB following approval of the revised SOW. We will recruit 40 women seeking oral contraceptives to be randomized to a low-dose progestin content oral contraceptive or a standard progestin content oral contraceptive and to have a breast biopsy after three month of oral contraceptive use. We will evaluate the effect of these progestin doses on genetic and cellular characteristics of the breast tissue.

The third protocol that is under development at this time involves obtaining breast biopsies from post-menopausal women who are receiving menopausal hormone therapy that contains micronized progesterone or placebo. The SOW will be revised to include this protocol and then will be submitted for IRB approval.

The protocol which is directly related to this Innovator Award, but not funded through it is our IRB-approved protocol which involves collecting breast tissue from women who have just had an induced abortion. This ‘pregnant’ breast tissue serves as an excellent comparator for the breast tissue that has been collected as part of Project 4 (see below) or will be collected as part of the three protocols described above.

As we continue to review the new literature and the results we generate we will develop additional protocols to further our understanding of how early pregnancy provides long-

term protection against breast cancer.

Task 2. Months 5-56: Recruit 48 nulliparous women to the treatment protocol.

We have revised the SOW to study a different group of women who do not have any breast abnormalities as an initial phase as we believe this will provide more generalizable results.

Task 3. Months 13-58: Assay tissue samples for hormonal, gene expression, and cellular markers to determine pre- and/or post-treatment tissue characteristics.

This work will begin in Month 30.

Task 4. Months 13-58: Assay blood samples for hormone levels.

This work will begin in Month 30.

Task 5. Months 14-60: Conduct data analysis to compare pre- and/or post-treatment tissue characteristics, to compare these changes to the differences noted between nulliparous and parous women, and to prepare manuscripts as appropriate.

This work will begin in Month 30.

Project 4

This project calls for the recruitment of 150 elective reduction mammoplasty patients. We will collect breast tissue from these women and conduct the same types of hormonal, genetic, and cellular analyses as will be done in Project 3. In addition, cellular analyses on 100 tissue slides from previous reduction mammoplasties will be conducted. In addition, cellular analyses will be conducted on 100 autopsy breast tissue samples. We are studying these three sources of breast tissue in parallel and thus describe our results to date together for these three tasks:

Task 1. Months 1-36: Recruit 150 women undergoing elective reduction mammoplasty to the protocol.

Task 1a. Months 1-36: Identify and conduct cellular assays on 100 tissue samples from previous reduction mammoplasties.

Task 1b. Months 23-48: Identify and conduct cellular assays on 100 autopsy breast tissue samples.

We have thus far enrolled 32 women in the prospective collection of tissue and reproductive questionnaire data from women undergoing elective reduction mammoplasties and are continuing to enroll subjects at the Pacific Surgery Center (Task

1). We have faced two related challenges with this protocol which have slowed recruitment considerably. The first is that our primary surgeon, Dr. Susan Downey, changed facilities in January 2006 and that process has resulted in fewer than anticipated subjects being enrolled as Dr. Downey built her practice. The second is that we needed to obtain new IRB approval with this change in facility and it took more than six months to receive IRB approval to collect tissue from Dr. Downey's new location. We are now on track and expect to collect tissue for four years rather than three years described in our year 1 annual report.

We are currently continuing to enroll women who previously had a reduction mammoplasty (Task 1a). We are actively working with 33 cases for whom we have detailed questionnaire data and were able to obtain tissue blocks of adequate quality.

We have obtained 100 autopsy breast tissue blocks from colleagues at the University of New Mexico (Task 1b).

To date, we have characterized ER expression, PR-A expression, PR-B expression, as well as quantified cell proliferation in the samples collected as part of Tasks 1 and 1a. We have also stained for smooth muscle actin, a myoepithelium marker, to allow us to determine whether PR-A is being expression only in luminal epithelial cells or if it is found in myoepithelium as well. Our next marker for evaluation is CD36. We have found some evidence that PR-A and PR-B expression are related in pre-menopausal women (see Figure 1 below), however there were no differences in PR isoform expression by parity status. ER-A expression was positively correlated with PR-A expression (p=0.006) in pre-menopausal women (see Figure 2 below) whereas no correlation was found between ER-A and PR-B. These comparisons include both tissue samples collected as part of task 1 and task 1a.

Figure 1. PR-A and PR-B expression in pre-menopausal reduction mammoplasty patients collected retrospectively and prospectively.

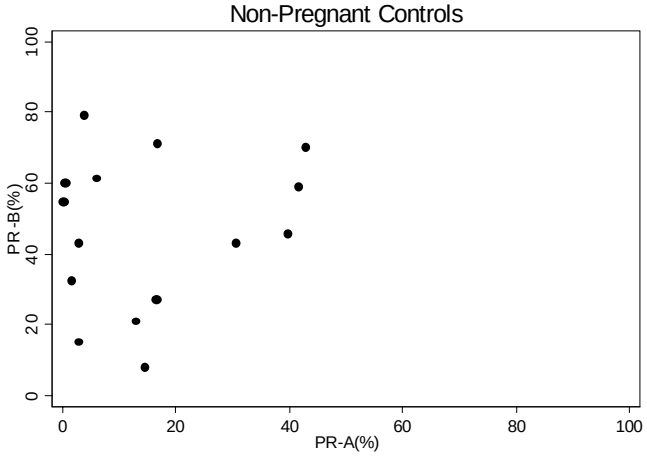

Figure 2. PR-A and ER-A expression in pre-menopausal reduction mammoplasty patients collected retrospectively and prospectively.

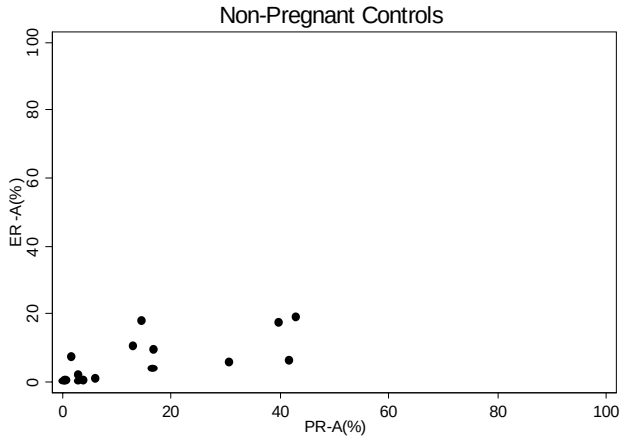

Task 2. Months 5-48: Assay tissue samples for hormonal and cellular markers to determine dense and non-dense tissue characteristics, and their association with glandular tissue proliferation.

The methods for assaying tissue hormone levels are still being evaluated. The protocol is clear for adipose tissue, however we have faced technical challenges in the laboratory and are continuing to work toward a protocol that can be used. The tissue samples collected for this purpose are frozen in the appropriate conditions and will be examined as soon as the methods are finalized.

Task 3. Months 5-48: Assay blood samples for hormone levels.

We are just beginning to conduct these assays. We plan to correlate serum estrogen and progesterone levels with breast cell proliferation and ER and PR expression with serum hormone measurements.

Task 4. Months 37-48: Conduct gene expression arrays on the dense and non-dense tissue samples to determine if the expression profiles differ.

Although this work is not set to begin until month 37, we have already made substantial progress in preparing to conduct gene expression arrays. In order to do this work properly, it is critical to isolate the relevant cell populations. This includes luminal epithelial cells, the stromal compartment, including fibroblasts, and adipocytes. We have developed a protocol for laser capture microscopy (LCM) to select out these specific cell types. It is critical that this be done with care and under the proper conditions to preserve the integrity of the RNA. We have successfully completed this process for one subject, ensured the quantity and integrity of the RNA and obtained expression levels for two genes using quantitative real-time PCR (qPCR) on the RNA extracted for this subject. We were able to obtain expression results for both a high abundance marker and a low abundance marker demonstrating the quality and quantity of the RNA we obtained. Because this is a time consuming, delicate effort we are now continuing LCM for all of

the samples collected through task 1. We anticipate that we will be on schedule for this task.

Task 5. Months 13-60: Conduct data analysis to compare dense and non-dense tissue characteristics and prepare manuscripts as appropriate.

We have sought to explore the role of collagen density in the breast tissue samples collected as part of tasks 1, 1a and 2. As reported last year, this work has already resulted in a seminal publication (Hawes *et al.*, *Breast Cancer Res* 8:R24-29, 2006). We have also performed immunostaining and *in situ* hybridization against collagens 1-5 and stained with Trichrome to visualize the general distribution of total collagens in dense and non-dense regions of normal human breast tissue from samples collected through tasks 1, 1a, and 1b. With these resources, we have analyzed tissue samples acquired from 89 patients to date.

We found that collagens 1 and 5 were present in human breast tissue but the relative ratio of collagen 1 to collagen 5 varied between specimens. Collagen 4 was also present in these human breast samples but only in the basement membrane surrounding the epithelium of all specimens. Its distribution did not change between specimens but it highlighted differences in the amount of epithelium present in each specimen. We believe that the amount of epithelium present may dictate the amount of collagen expressed in the breast and with parity the epithelium may apoptose and the surrounding collagen may shrink as the signal coming from the epithelium is no longer there to sustain collagen expression.

Since the collagens are located in the extracellular matrix we wanted to know which cells were synthesizing and secreting them. For this purpose we detected collagen 1 and 5 encoding RNAs by *in situ* hybridization. The distribution suggested that it was expressed in both epithelium and stromal cells, but not in every cell. This idea is novel, since most experiments are performed on cell lines and not examined in whole tissue. Our data suggests that the signal to express certain collagens is coming not only from the stroma as previously thought, but also from the epithelium.

KEY RESEARCH ACCOMPLISHMENTS:

- Treatment of rats with hormonal chemoprevention regimens and determination of effective regimens.
- Evaluation of rat mammary gland morphology.
- Identification of genes expressed in a parity-specific manner in multiple rat strains resulting in a key publication in *Cancer Research* (Blakely *et al.*, 2006, see Appendix).
- Development of a novel research protocol to allow us to evaluate the appropriateness of a progestin-based breast cancer chemopreventive approach.
- Development and initiation of a research protocol to collect interview data, tissue specimens, and mammograms on women having elective reduction mammoplasties.
- Development of a novel research protocol to allow us to evaluate breast cell proliferation in women receiving different progestin-dose oral contraceptives.
- Development of a novel research protocol to allow us to evaluate breast cell proliferation in women receiving micronized progesterone versus placebo to determine the effect of exogenous progesterone on proliferation.
- Discovery that collagen is produced in both stromal and epithelial cells.
- Evaluation of tissue samples from previous reduction mammoplasties resulting in a seminal publication in *Breast Cancer Research* (Hawes *et al.*, 2006, see Appendix).
- Contact and interview 35 previous reduction mammoplasty subjects to obtain demographic, reproductive, and hormone use data.
- Staining and evaluation of ER-A, PR-A, and PR-B expression and cell proliferation in previous reduction mammoplasty samples and prospective reduction mammoplasty samples.
- Development of methods for laser capture microscopy to isolate relevant cell populations.
- Successful RNA extraction, quantitation and integrity evaluation from LCM sample followed by quantitative gene expression measurement of both high and low abundance markers.
- Continued development of methods for assaying hormone levels in dense (stromal) tissue.
- A further key accomplishment is the development of a network of collaborators at USC and across the United States to further the work being funded by this grant.
    - At USC we have formed a working group of investigators with expertise in endocrinology, gynecology, breast cancer pathology, oncology, radiology, epidemiology and molecular biology/embryology who meet at least twice a month to review progress of the various projects and specific related tasks and to discuss any data generated from the studies and any new questions that may arise from our studies or published literature. An important new research protocol to obtain breast tissue biopsies from women who were very recently pregnant has been approved by the USC IRB and is underway. The sample set of 35 breast tissue samples obtained through this protocol represents the largest collection of tissue samples

from the pregnant breast (or recently pregnant). Although this work is funded through other mechanisms it is a direct off-shoot of the meetings held to further the goals of this research grant.

- We have also sought out a number of investigators with similar interests in breast cancer across the United States. We are now collaborating with Dr. Sue Bartow and Dr. Dorothy Pathak to perform cellular marker analysis on breast specimens from autopsies performed in New Mexico. These are the same specimens utilized by Dr. Norman Boyd's group (Li *et al.*, *Cancer Epidemiol Biomarkers Prev* 14:343-349, 2005). Although this work is not currently funded through this grant it also came about as a direct result of planning to meet the goals of this grant.
- As part of this grant, we have had meetings with Dr. Dan Medina and his colleagues at Baylor, and with Dr. Satyabrata Nandi and his colleagues at UC Berkley to ensure that we were aware of their current thinking regarding chemoprevention in rodents.
- Dr. Charlotte Kuperwasser of Tufts University and Dr. Pepper Schedin of the University of Colorado have both visited and we now have ongoing scientific discussions with these leading investigators.

REPORTABLE OUTCOMES:

1. Blakely CM, Stoddard AJ, Belka GK, Dugan KD, Notarfrancesco KL, Moody SE, D'Cruz CM, and Chodosh LA. Hormone-induced protection against mammary tumorigenesis is conserved in multiple rat strains and identifies a core gene expression signature induced by pregnancy. *Cancer Research*, 66:6421-6431, 2006.
2. Hawes D, Downey S, Pearce CL, Bartow S, Wan P, Pike MC, Wu AH. Dense breast stromal tissue shows greatly increased concentration of breast epithelium but no increase in its proliferative activity. *Breast Cancer Res*, 8:R24-29, 2006.

CONCLUSION:

The successful identification of a set of breast tissue gene expression differences (changes) that distinguish parous from nulliparous rats of multiple strains (and confirmed in a strain of mice) is a critical step in our development of a chemoprevention approach to mimic the protective effect of pregnancy. If we can confirm these genetic expression changes in rodents treated with a variety of hormonal chemoprevention regimens (part of our current work) and also confirm them in women (part of our current work), they should provide a critical biomarker of effect for chemoprevention approaches in women that attempt to mimic the protective effect of pregnancy.

Our finding that breast epithelial tissue in women is overwhelmingly concentrated in mammographically dense areas of the breast (areas of high collagen concentration not seen in rodent breast) provides a deep insight into the reason for increased mammographic density being so closely associated with increased risk of breast cancer - women with increased mammographic density have more breast epithelium. The reason(s) for this relationship is at present unclear and is a focus of our current research. Breast densities are reduced in parous compared to nulliparous women, so that this endeavor ties in closely with our development of a chemoprevention regimen to mimic the protective effect of pregnancy. It may be that the genetic expression changes brought about by pregnancy (discussed above) are themselves responsible for the reduction in densities. We hope through the protocols we have developed to test Dr. Chodosh's findings in the rat and if they are confirmed we can proceed to test the chemoprevention agents identified to be effective in the rat.

In addition, through our successful development of a laser capture microscopy protocol we will be able to conduct large scale gene expression studies on the relevant breast cell populations over the next six months which will refine our understanding of the result obtained in Dr. Chodosh's rodent experiments and provide further insight into the characteristics of the parous breast which ultimately provides protection against breast cancer.

REFERENCES:

1. Blakely CM, Stoddard AJ, Belka GK, Dugan KD, Notarfrancesco KL, Moody SE, D'Cruz CM, and Chodosh LA. Hormone-induced protection against mammary tumorigenesis is conserved in multiple rat strains and identifies a core gene expression signature induced by pregnancy. *Cancer Research*, 66:6421-6431, 2006.
2. Hawes D, Downey S, Pearce CL, Bartow S, Wan P, Pike MC, Wu AH. Dense breast stromal tissue shows greatly increased concentration of breast epithelium but no increase in its proliferative activity. *Breast Cancer Res*, 8:R24-29, 2006.
3. Li T, Sun L, Miller N, Nicklee T,Woo J,Hulse-Smith L,Tsao MS,Khokha R, Martin L, Boyd N. *Cancer Epidemiol Biomarkers Prev*, 14:343-349, 2005.

APPENDICES:

1. Blakely CM, Stoddard AJ, Belka GK, Dugan KD, Notarfrancesco KL, Moody SE, D'Cruz CM, and Chodosh LA. Hormone-induced protection against mammary tumorigenesis is conserved in multiple rat strains and identifies a core gene expression signature induced by pregnancy. *Cancer Research*, 66:6421-6431, 2006.
2. Hawes D, Downey S, Pearce CL, Bartow S, Wan P, Pike MC, Wu AH. Dense breast stromal tissue shows greatly increased concentration of breast epithelium but no increase in its proliferative activity. *Breast Cancer Res*, 8:R24-29, 2006.
3. List of personnel

Hormone-Induced Protection against Mammary Tumorigenesis Is Conserved in Multiple Rat Strains and Identifies a Core Gene Expression Signature Induced by Pregnancy

Collin M. Blakely, Alexander J. Stoddard, George K. Belka, Katherine D. Dugan, Kathleen L. Notarfrancesco, Susan E. Moody, Celina M. D'Cruz, and Lewis A. Chodosh

Departments of Cancer Biology, Cell and Developmental Biology, and Medicine, and The Abramson Family Cancer Research Institute, University of Pennsylvania School of Medicine, Philadelphia, Pennsylvania

Abstract

Women who have their first child early in life have a substantially lower lifetime risk of breast cancer. The mechanism for this is unknown. Similar to humans, rats exhibit parity-induced protection against mammary tumorigenesis. To explore the basis for this phenomenon, we identified persistent pregnancy-induced changes in mammary gene expression that are tightly associated with protection against tumorigenesis in multiple inbred rat strains. Four inbred rat strains that exhibit marked differences in their intrinsic susceptibilities to carcinogen-induced mammary tumorigenesis were each shown to display significant protection against methylnitrosourea-induced mammary tumorigenesis following treatment with pregnancy levels of estradiol and progesterone. Microarray expression profiling of parous and nulliparous mammary tissue from these four strains yielded a common 70-gene signature. Examination of the genes constituting this signature implicated alterations in transforming growth factor-β signaling, the extracellular matrix, amphiregulin expression, and the growth hormone/insulin-like growth factor I axis in pregnancy-induced alterations in breast cancer risk. Notably, related molecular changes have been associated with decreased mammographic density, which itself is strongly associated with decreased breast cancer risk. Our findings show that hormone-induced protection against mammary tumorigenesis is widely conserved among divergent rat strains and define a gene expression signature that is tightly correlated with reduced mammary tumor susceptibility as a consequence of a normal developmental event. Given the conservation of this signature, these pathways may contribute to pregnancy-induced protection against breast cancer. (Cancer Res 2006; 66(12): 6421-31)

Introduction

Epidemiologic studies clearly show that a woman's risk of developing breast cancer is influenced by reproductive endocrine events (1). For example, early age at first full-term pregnancy, as well as increasing parity and duration of lactation, have each been shown to reduce breast cancer risk (2, 3). In particular, women who have their first child before the age of 20 have up to a 50% reduction in lifetime breast cancer risk compared with their nulliparous counterparts (2). Notably, the protective effects of an early full-term pregnancy have been observed in multiple ethnic groups and geographic locations, suggesting that parity-induced protection results from intrinsic biological changes in the breast rather than specific socioeconomic or environmental factors. At present, however, the biological mechanisms underlying this phenomenon are unknown.

Several models to explain the protective effects of parity have been proposed. For instance, parity has been hypothesized to induce the terminal differentiation of a subpopulation of mammary epithelial cells, thereby decreasing their susceptibility to oncogenesis (4). Related to this, parity has been suggested to induce changes in cell fate within the mammary gland, resulting in a population of mammary epithelial cells that are more resistant to oncogenic stimuli by virtue of decreased local growth factor expression and/or increased transforming growth factor (Tgf)-β3 and p53 activity (5, 6). Others have suggested that the process of involution that follows pregnancy and lactation acts to eliminate premalignant cells or cells that are particularly susceptible to oncogenic transformation (5). Conversely, parity-induced decreases in breast cancer susceptibility could also be due to persistent changes in circulating hormones or growth factors rather than local effects on the mammary gland (7). At present, however, only limited cellular or molecular evidence exists to support any of these models.

Similar to humans, both rats and mice exhibit parity-induced protection against mammary tumorigenesis. Administration of the chemical carcinogens, 7,12-dimethylbenzanthracene or methylnitrosourea, to nulliparous rats results in the development of hormone-dependent mammary adenocarcinomas that are histologically similar to human breast cancers (8). In outbred Sprague-Dawley, and inbred Lewis and Wistar-Furth rats, a full-term pregnancy either shortly before or after carcinogen exposure results in a high degree of protection against mammary carcinogenesis (7, 9, 10). Similarly, treatment of rats with pregnancy-related hormones, such as 17-β-estradiol (E) and progesterone (P), can mimic the protective effects of pregnancy in rat mammary carcinogenesis models (11, 12). This suggests that the mechanisms of parity-induced protection and estradiol and progesterone–induced protection may be similar. Using analogous approaches, Medina and colleagues have shown parity-induced as well as hormone-induced protection against 7,12-dimethylbenzanthracene–initiated carcinogenesis in mice (13, 14). As such, rodent models recapitulate the ability of reproductive endocrine events to modulate breast cancer risk as observed in humans. This, in turn, permits the mechanisms of parity-induced protection to be studied within defined genetic and reproductive contexts.

Requests for reprints: Lewis A. Chodosh, Department of Cancer Biology, University of Pennsylvania School of Medicine, 612 Biomedical Research Building II/III, 421 Curie Boulevard, Philadelphia, PA 19104-6160. Phone: 215-898-1321; Fax: 215-573-6725; E-mail: chodosh@mail.med.upenn.edu.

doi:10.1158/0008-5472.CAN-05-4235

Previously, analyses of gene expression changes that occur in rodent models in response to parity, or hormonal treatments that mimic parity, have been used to suggest potential cellular and molecular mechanisms for pregnancy-induced protection against breast cancer (6, 15). Rosen and colleagues used subtractive hybridization analysis to identify genes in the mammary glands of Wistar-Furth rats that were persistently up-regulated 4 weeks posttreatment with estradiol and progesterone (15). Estradiol and progesterone treatment was found to increase the mRNA expression of a wide range of genes, including those involved in differentiation, cell growth, and chromatin remodeling. Similarly, we used microarray expression profiling to assess global gene expression changes induced by parity in the mammary glands of FVB mice (6). This analysis revealed parity-induced increases in epithelial differentiation markers, *Tgfb3* and its downstream targets, and cellular markers reflecting the influx of macrophages and lymphocytes into the parous gland. We also found that parity resulted in persistent decreases in the expression of a number of growth factor–encoding genes, including amphiregulin (*Areg*) and insulin-like growth factor (*Igf-I*). Together, these studies provided initial insights into cellular and molecular mechanisms that could contribute to parity-induced protection.

Notably, early first full-term pregnancy in humans primarily decreases the incidence of estrogen receptor (ER)-positive breast cancers (16). Because rats are more similar to humans than are mice with respect to the incidence of ER-positive mammary tumors (17), in the present study we used microarray expression profiling to identify persistent gene expression changes in the mammary glands of this rodent species to explore potential mechanisms of parity-induced protection. To date, a comprehensive analysis of parity-induced up-regulated and down-regulated gene expression changes in the rat has not been performed.

A major challenge posed by global gene expression surveys is the large number of differentially expressed genes that are typically identified, only a few of which may contribute causally to the phenomenon under study. Consequently, we considered approaches to identifying parity-induced changes in the rat mammary gland that would permit the resulting list of expressed genes to be narrowed to those most robustly associated with parity-induced protection against mammary tumorigenesis. Given the marked genetic and biological heterogeneity between different inbred rat strains, we reasoned that identifying expression changes that are conserved across multiple strains exhibiting hormone-induced protection against mammary tumorigenesis would facilitate the identification of a core set of genes associated with parity-induced protection against breast cancer.

To achieve this goal, we focused on gene expression changes that are conserved among different strains of rats that exhibit hormone-induced protection against mammary tumorigenesis. We first identified four genetically distinct inbred rat strains that exhibit hormone-induced protection against methylnitrosourea-induced mammary tumorigenesis independent of their inherent susceptibility to this carcinogen. We then used oligonucleotide microarrays to identify a core 70-gene expression signature that closely reflects parity-induced changes in the mammary gland that were conserved among each of these strains. The results of this analysis extend prior observations with respect to parity-induced changes in the growth hormone/Igf-I axis, identify novel parity-induced changes associated with the extracellular matrix (ECM), and implicate a core set of pathways in pregnancy-induced protection against breast cancer.

Materials and Methods

Animals and tissues. Lewis, Wistar-Furth, Fischer 344, and Copenhagen rats (Harlan, Indianapolis, IN) were housed under 12-hour light/12-hour dark cycles with access to food and water ad libitum. Animal care was performed according to institutional guidelines. To generate parous (G1P1) rats, 9-week-old females were mated and allowed to lactate for 21 days after parturition. After 28 days of postlactational involution, rats were sacrificed by carbon dioxide asphyxiation and the abdominal mammary glands were harvested and snap-frozen following lymph node removal, or whole-mounted and fixed in 4% paraformaldehyde. Whole-mounted glands were stained with carmine alum as previously described (6). For histologic analysis of whole mammary glands and tumors, paraffin-embedded tissues were sectioned and stained with H&E or Mason's trichrome as previously described (6). Tissues were harvested from age-matched nulliparous (G0P0) animals in an identical manner.

Carcinogen and hormone treatments. Twenty-five to 30 nulliparous female Lewis, Fischer 344, Wistar-Furth, and Copenhagen rats were weighed and treated at 7 weeks of age with methylnitrosourea (Sigma-Aldrich, St. Louis, MO) at a dose of 50 mg/kg by a single i.p. injection. At 9 weeks of age, animals from each strain were assigned to one of two groups and treated with hormone pellets (Innovative Research, Sarasota, FL) by s.c. implantation. Group 1 received pellets containing 35 mg of 17-β-estradiol + 35 mg of progesterone, whereas group 2 received pellets containing placebo. Pellets were removed after 21 days of treatment. No signs of toxicity were observed. The development of mammary tumors was assessed by weekly palpation. Animals were sacrificed at a predetermined tumor burden, or at 60 weeks postmethylnitrosourea. At sacrifice, all mammary glands were assessed for tumors, which were fixed in 4% paraformaldehyde and embedded in paraffin. Tumor samples from each strain were confirmed as carcinomas by histologic evaluation. Statistical differences in tumor-free survival between experimental groups were determined by log rank tests and by the generation of hazard ratios (HR) based on the slope of the survival curves using GraphPad Prism 4.0 software.

Microarray analysis. RNA was isolated from snap-frozen abdominal mammary glands by the guanidine thiocyanate/cesium chloride method as previously described (6). Ten micrograms of total RNA from individual Wistar-Furth (six G0P0 and five G1P1), Fischer 344 (eight G0P0 and six G1P1), and Copenhagen (six G0P0 and five G1P1) rats was used to generate cDNA and biotinylated cRNA as previously described (6). For Lewis rats, three G0P0 and three G1P1 samples were analyzed, each of which was comprised of 10 μg of pooled RNA from three animals. To permit the identification of epithelial as well as stromal gene expression changes, intact mammary glands (with lymph nodes removed) were used. Samples were hybridized to high-density oligonucleotide microarrays (RGU34A) containing ~8,800 probe sets representing ~4,700 genes and expressed sequence tags. Affymetrix comparative algorithms (MAS 5.0) and Chipstat were used to identify genes that were differentially expressed between nulliparous and parous samples (18). Robust Multichip Average signal values were generated using Bioconductor (19).

Genes were selected for further analysis whose expression changed significantly by the above analysis in three out of four strains. Significance was assessed by randomly generating eight lists equal in size to the up-regulated and down-regulated lists for each strain from the population of nonredundant genes called present on the chip in at least one sample (2,428 genes). One million random draw trials were performed to calculate a nominal *P* value for combined list length and to estimate the false discovery rate (FDR) using the median list size occurring by chance.

Hierarchical clustering was done using R statistical software[1] and as described (20). Mouse genes were identified using the Homologene database (National Center for Biotechnology Information).

Quantitative real-time PCR. Five micrograms of DNase-treated RNA were used to generate cDNA by standard methods. *Csn2, Mmp12, Tgfb3,*

[1] http://www.R-project.org.

Igfbp5, Areg, Igf-I, Ghr, Serpinh1, and *Sparc* were selected for confirmation by quantitative real-time PCR (QRT-PCR) using TaqMan assays (Applied Biosystems, Foster City, CA). *B2m* was used as a control (21, 22). Reactions were performed in duplicate in 384-well microtiter plates in an ABI Prism Sequence Detection System according to standard methods (Applied Biosystems). One-tailed *t* tests were performed to determine statistical significance using Prism 4.0 software.

Results

Hormone-induced protection in inbred rat strains. To determine whether hormone-induced protection against mammary tumorigenesis is a feature unique to carcinogen-sensitive strains, we compared the extent of protection induced by hormones in four different rat strains: Lewis, Wistar-Furth, Fischer 344, and Copenhagen. Two of these strains (Lewis and Wistar-Furth) have been reported to exhibit hormone-induced protection (9, 12). However, it has not been determined whether carcinogen-resistant strains of rats, such as Copenhagen (23), also exhibit protection. Female rats from each strain were treated with a single dose of methylnitrosourea at 7 weeks of age, followed by s.c. implantation of either placebo or hormone pellets (35 mg of estradiol + 35 mg of progesterone) at 9 weeks of age. Among the placebo-treated groups, Lewis rats exhibited the highest susceptibility to methylnitrosourea-induced mammary tumorigenesis with 100% penetrance and a median tumor latency of 13 weeks (Fig. 1*A*). Fischer 344 and Wistar-Furth rats displayed intermediate carcinogen sensitivity with latencies of 24 and 36 weeks, respectively. In contrast, Copenhagen rats exhibited a high degree of resistance to methylnitrosourea-induced mammary tumorigenesis with only 5 of 12 animals developing mammary tumors, with an average latency of 51 weeks.

Surprisingly, despite the wide variance in carcinogen sensitivity of nulliparous rats from these four strains, estradiol and progesterone treatment induced a significant ($P < 0.05$) degree of protection against mammary tumorigenesis in each strain (Fig. 1*B*). For example, whereas Lewis and Copenhagen strains differed markedly in their sensitivity to methylnitrosourea, they exhibited strikingly similar degrees of hormone-induced protection with HRs of 0.19 [95% confidence interval (CI), 0.05-0.40] and 0.16 (95% CI, 0.02-0.63), respectively. The Wistar-Furth (HR, 0.31; 95% CI, 0.09-0.90) and Fischer 344 (HR, 0.38; 95% CI, 0.10-0.71) strains exhibited lesser, but significant degrees of protection. These experiments show that hormone treatments that mimic pregnancy confer protection against mammary tumorigenesis in each strain irrespective of the intrinsic carcinogen susceptibility of nulliparous animals from that strain.

Morphologic changes induced by parity in the rat mammary gland. Parity-induced changes in breast cancer susceptibility have been reported to be accompanied by persistent changes in the structure of the mammary gland in humans, as well as in rats and mice (4, 6). Consistent with this, carmine-stained whole-mount analysis of nulliparous and parous mammary glands from each of the four rat strains revealed that the architecture of the parous mammary epithelial tree was more complex than that of age-matched nulliparous animals, with a higher degree of ductal side-branching (Fig. 1*C*). These effects were observed in each of the four strains analyzed, suggesting that changes in the structural and cellular composition of the mammary gland may occur as a consequence of parity.

Microarray analysis of parity-induced changes in the rat mammary gland. The similar morphologic changes induced by parity suggested that the hormone-induced protection against mammary tumorigenesis that we observed in different rat strains might be accompanied by common molecular alterations. To identify these changes, we first performed oligonucleotide microarray expression profiling on pooled samples from nulliparous and parous Lewis rats. Genes whose expression changes were considered to be statistically significant using established algorithms, and whose expression changed by at least 1.2-fold as a result of parity, were selected for further analysis (18). This combined analytic approach has previously been shown to be capable of identifying differentially expressed genes with high sensitivity and specificity (18). Gene expression analysis performed in this manner identified 75 up-regulated and 148 down-regulated genes in parous compared with nulliparous mammary glands. Examination of this list of differentially expressed genes confirmed our previous findings in mice that parity results in the persistent up-regulation of *Tgfb3*, as well as differentiation and immune markers, as well as the persistent down-regulation of growth factor encoding genes, such as *Areg* and *Igf-I* (ref. 6; data not shown).

To narrow the list of candidate genes whose regulation might contribute to the protected state associated with parity, we attempted to identify parity-induced gene expression changes that were conserved across multiple rat strains. To this end, total RNA was isolated from the mammary glands of nulliparous and parous Wistar-Furth, Fischer 344, and Copenhagen rats, and analyzed on RGU34A arrays in a manner analogous to that employed for Lewis rats. This led to the identification of 68, 64, and 92 parity up-regulated genes and 132, 209, and 149 parity down-regulated genes in Wistar-Furth, Fischer 344, and Copenhagen rats, respectively.

Unsupervised hierarchical clustering performed using the expression profiles of 1,954 globally varying genes across the nulliparous and parous data sets representing the four rat strains revealed that samples clustered primarily based on strain without regard to parity status (Fig. 2*A*). This suggested that the principal source of global variation in gene expression across these data sets was due to genetic differences between strains rather than reproductive history. This observation suggested that determining which parity-induced gene expression changes were conserved among these highly divergent rat strains could represent a powerful approach to defining a parity-related gene expression signature correlated with hormone-induced protection against mammary tumorigenesis.

To identify parity-induced gene expression changes that were conserved across strains, we selected genes that exhibited $\geq$1.2-fold change in at least three of the four strains analyzed. This led to the identification of 24 up-regulated (Table 1) and 46 down-regulated genes (Table 2). Based on the number of parity-induced gene expression changes observed for each strain, an overlap of this size is highly unlikely by chance (up-regulated: $P < 1 \times 10^{-6}$, FDR < 1%; down-regulated: $P < 1 \times 10^{-6}$, FDR = 4%). As such, this approach led to the identification of 70 genes whose expression is persistently altered by parity across multiple strains of rats that exhibit hormone-induced protection against mammary tumorigenesis.

A gene expression signature distinguishes parous and nulliparous rats and mice. To confirm the validity of the 70-gene parity-related expression signature derived from the above studies, we performed oligonucleotide microarray analysis on samples from nulliparous and parous Lewis rats that were generated independently from those used to derive this signature. Hierarchical clustering analysis of these independent samples using the 70-gene signature revealed that the expression profiles of these genes were sufficient to accurately distinguish parous from nulliparous Lewis rat samples in a blinded manner (Fig. 2*B*).

To determine whether this parity-related signature could distinguish between nulliparous and parous mammary glands from multiple strains of rats, Lewis, Wistar-Furth, Fischer 344, and Copenhagen microarray data sets were clustered in an unsupervised manner based solely on the expression of the 70 genes comprising the parity signature (Fig. 2*C*). In each of the four rat strains examined, the 70-gene signature was sufficient to distinguish parous from nulliparous rats (Fig. 2*C*). Thus, this signature reflects parity-induced gene expression changes that are highly conserved among four genetically divergent rat strains.

Early full-term pregnancy has been reported to result in protection against mammary tumorigenesis in mice, as it does in humans and rats (13). Accordingly, we mapped the 70 genes

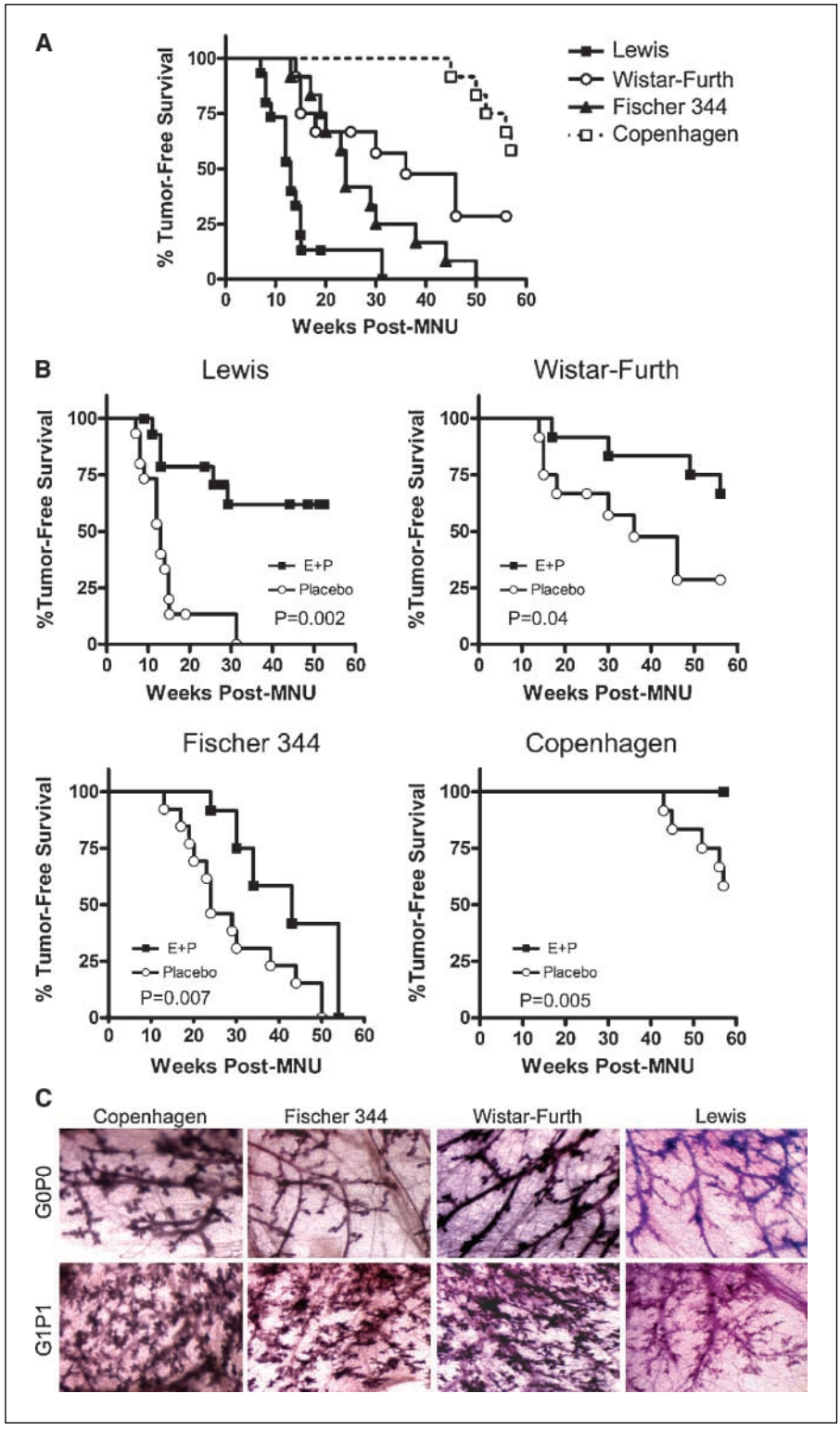

Figure 1. Hormone-induced protection against mammary tumorigenesis is conserved among multiple rat strains. *A,* Kaplan-Meier curves plotting the time to the formation of a first mammary tumor in placebo-treated groups for Lewis (n = 15), Wistar-Furth (n = 12), Fischer 344 (n = 13), and Copenhagen (n = 12) rats treated with methylnitrosourea (*MNU*) at 7 weeks of age. Significant differences in tumor incidence were identified between Lewis and Wistar-Furth (P = 0.0003), Lewis and Fischer 344 (P = 0.0005), Lewis and Copenhagen (P = 0.0001), Wistar-Furth and Copenhagen (P = 0.024), and Fischer 344 and Copenhagen (P = 0.0001) as determined by a log rank test. Wistar-Furth and Fischer 344 were not significantly different (P = 0.14). *B,* mammary tumor incidence for placebo and estradiol and progesterone–treated rats is plotted for each strain. Cohort sizes for estradiol and progesterone–treated animals were: Lewis (n = 16), Wistar-Furth (n = 12), Fischer 344 (n = 12), and Copenhagen (n = 12). Each strain exhibited significantly decreased tumor incidence in estradiol and progesterone–treated compared with placebo-treated cohorts. *C,* carmine-stained whole mounts of abdominal mammary glands from nulliparous (G0P0) and parous (G1P1) rats from each strain (original magnification, ×50). Samples are representative of three animals per group.

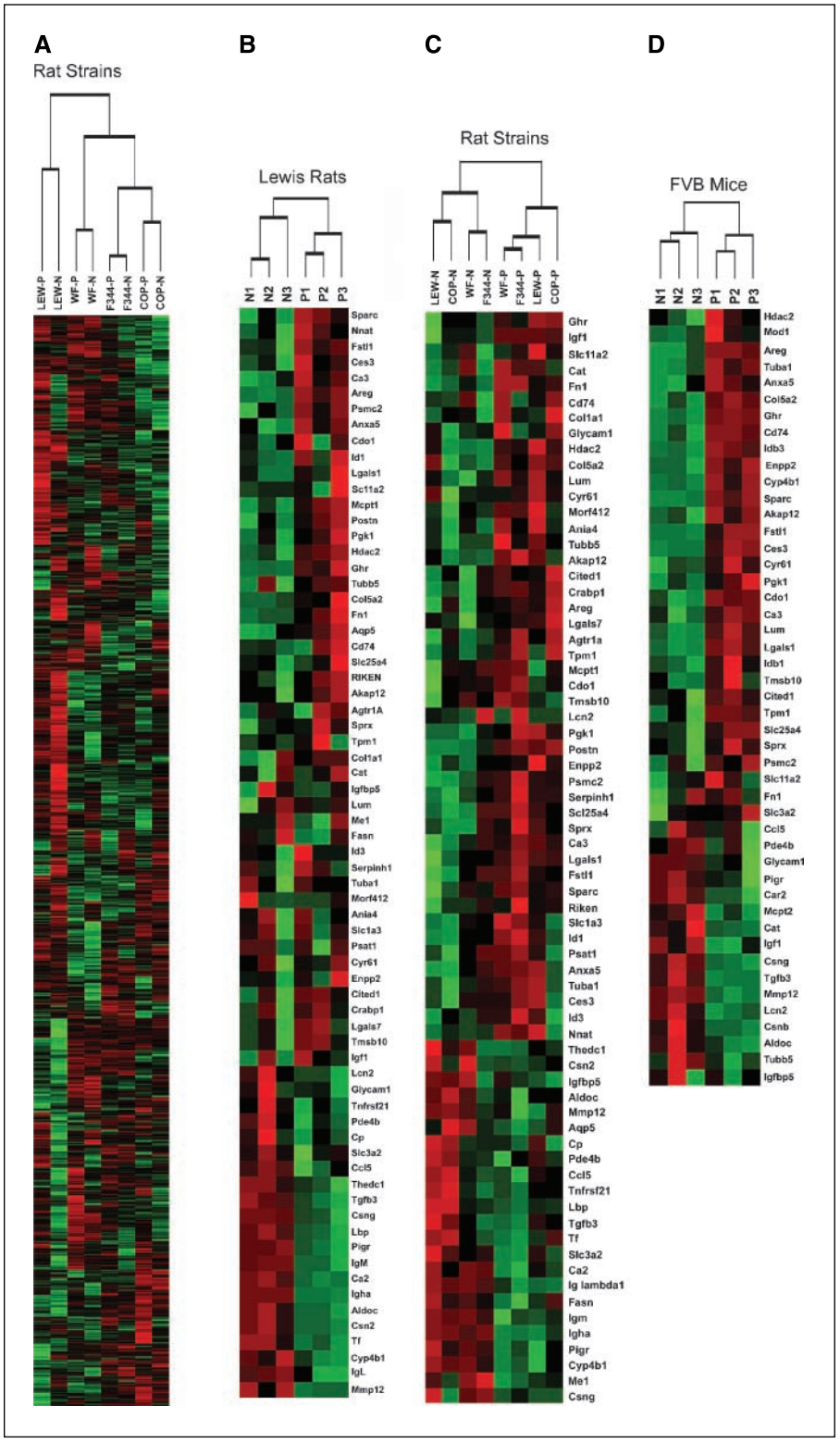

Figure 2. A parity-related gene expression signature distinguishes between nulliparous and parous rats and mice. Unsupervised hierarchical clustering analysis. Nulliparous (*N*), parous (*P*), Lewis (*LEW*), Fischer 344 (*F344*), Wistar-Furth (*WF*), and Copenhagen (*COP*). *A,* nulliparous and parous samples from each strain were clustered based on the median expression values of ~1,900 genes exhibiting global variation in gene expression across the data sets. *B,* six independent Lewis samples [three nulliparous (N1-N3) and three parous (P1-P3)] were clustered based solely on the expression of genes in the 70-gene parity signature. *C,* clustering analysis based solely on the expression of the 70-gene parity signature was performed on nulliparous and parous samples from Lewis, Wistar-Furth, Fischer, and Copenhagen rats. *D,* the 70-gene rat parity signature was mapped to the mouse genome using Homologene, yielding 47 mouse genes. Six FVB mouse samples [three nulliparous (N1-N3) and three parous (P1-P3)] were clustered based on the expression profiles of these 47 genes.

constituting the rat parity signature to the mouse genome, and assessed their expression profiles in nulliparous and parous FVB mouse mammary samples. Of the 70 genes that were mapped, 47 were represented on Affymetrix MGU74Av2 microarrays. These 47 genes were sufficient to distinguish nulliparous from parous samples in a blinded manner (Fig. 2*D*). Thus, a parity-related gene expression signature generated in the rat is able to predict reproductive history in the mouse, suggesting that the persistent molecular alterations that occur in response to parity are conserved across rodent species.

Among the 70 genes that we identified as being consistently regulated by parity, at least five categories were evident.

Table 1. Genes up-regulated in parous rats

Gene name	Symbol	Gene ID	Function	Category	Fold-change G1P1 versus G0P0				
					Lewis	WF	F344	Cop	Median
Immunoglobulin heavy chain	*Igha*	314487	Immunoglobulin	Immune	39.4	25.4	4.5	6.9	25.4
Casein β	*Csn2*	29173	Milk protein	Differentiation	8.0	5.2	1.9	1.5	5.2
IgM light chain		287965	Immunoglobulin	Immune	2.5	3.8	1.8	1.6	2.5
Matrix metalloproteinase 12	*Mmp12*	117033	Proteolysis	ECM/Immune	2.6	1.4	2.0	1.3	2.0
Casein γ	*Csng*	114595	Milk protein	Differentiation	3.1	1.9	1.2	0.9	1.9
Fatty acid synthase	*Fasn*	50671	Fatty acid biosynthesis	Metabolism/ differentiation	2.0	1.6	1.7	0.9	1.7
Cytochrome P450, family 4, subfamily b,1	*Cyp4b1*	24307	Monooxygenase activity	Metabolism	1.6	1.5	1.2	1.2	1.5
Carbonic anhydrase 2	*Ca2*	54231	Carbon dioxide hydration	Metabolism	1.5	1.5	1.4	1.1	1.5
Ig lambda-1 chain C region		363828	Immunoglobulin	Immune	1.5	1.4	1.4	1.3	1.4
Malic enzyme 1	*Me1*	24552	Pyruvate synthesis	Metabolism	1.3	1.4	1.4	1.1	1.4
Insulin-like growth factor binding protein 5	*Igfbp5*	25285	Igf-I-binding	Growth factor/ ECM	2.4	1.4	0.9	2.7	1.4
Lipopolysaccharide binding protein	*Lbp*	29469	Antibacterial	Immune	2.1	1.3	1.4	2.0	1.4
Polymeric immunoglobulin receptor	*Pigr*	25046	Trancytosis	Immune	1.7	1.4	1.2	1.1	1.4
Transforming growth factor, β3	*Tgfb3*	25717	Cell growth/ proliferation	Tgf-β	1.5	1.3	1.2	1.4	1.3
Aquaporin 5	*Aqp5*	25241	Water transport	Transporter	1.3	1.7	1.2	1.5	1.3
Phosphodiesterase 4B	*Pde4b*	24626	Cyclic AMP phoshodiesterase	Signal transduction	1.3	1.4	1.0	1.4	1.3
Thioesterase domain containing 1	*Thedc1*	64669	Fatty acid biosynthesis	Metabolism/ differentiation	1.9	1.2	1.3	1.5	1.3
Transferrin	*Tf*	24825	Iron transport	Transport/ differentiation	1.4	1.2	1.3	1.5	1.3
Ceruloplasmin	*Cp*	24268	Copper transport	Transport/ differentiation	1.3	1.0	1.2	2.2	1.2
Similar to death receptor 6	*Tnfrsf21*	316256	Apoptosis	Signal transduction	1.3	1.0	1.2	1.3	1.2
Aldolase C, fructose-biphosphate	*Aldoc*	24191	Fructose metabolism	Metabolism	1.2	1.2	1.1	1.3	1.2
Lipocalin 2	*Lcn2*	170496	Iron binding/antibacterial	Immune	1.3	1.1	1.2	1.4	1.2
Solute carrier family 3, member 2	*Slc3a2*	50567	Amino acid transporter	Transporter	1.2	1.1	1.2	1.3	1.2

NOTE: Genes identified as up-regulated by at least 1.2-fold in three out of four rat strains as a result of parity are reported from the highest to lowest median fold change. Gene names and symbols are reported based on the Rat Genome Database, and Gene ID according to Entrez Gene. Gene functions and categories are based on Gene Ontology.
Abbreviations: WF, Wistar-Furth; F344, Fischer 344; Cop, Copenhagen.

These included the previously identified differentiation, immune, Tgf-β, and growth factor categories (6), as well as an additional category of genes that are involved in ECM structure and function (Tables 1 and 2). We previously showed that clustering based on genes in each of the first four categories was sufficient to distinguish between nulliparous and parous rats (6). In an analogous manner, we tested whether unsupervised clustering based solely on ECM-related genes would be sufficient to differentiate between nulliparous and parous rat or mouse samples. In each case, ECM-related gene expression patterns alone were sufficient to distinguish between nulliparous and parous mammary samples from the four different rat strains (Fig. 3*A*), from independent mammary samples derived from nulliparous and parous Lewis rats (Fig. 3*B*), and from mammary samples derived from FVB mice (Fig. 3*C*). This indicates that differential expression of a subset of genes involved in ECM structure and function represents a conserved feature of parity-induced changes in the rodent mammary gland.

Parity up-regulates *Tgfb3* and expression of differentiation and immune markers. Our previous analysis of parity-induced gene expression changes in FVB mice was consistent with the parity-induced up-regulation of Tgf-β3 activity. Similarly, in the current study, we found that *Tgfb3* expression was up-regulated by parity in each of the four rat strains examined (Table 1). This finding was confirmed by QRT-PCR

Table 2. Genes down-regulated in parous rats

Gene name	Symbol	Gene ID	Function	Category	Fold-change G1P1 versus G0P0				
					Lewis	WF	F344	Cop	Median
Periostin	*Postn*	361945	Transcription factor	Differentiation	1.9	2.1	1.8	2.2	2.0
Amphiregulin	*Areg*	29183	Epidermal growth factor receptor ligand	Growth factor	3.5	2.1	1.7	1.9	2.0
Cellular retinoic acid binding protein I	*Crabp1*	25061	Retinoic acid receptor signaling	Signal transduction	1.8	2.1	1.3	1.5	1.7
Insulin-like growth factor 1	*Igf-I*	24482	Cell proliferation/ survival	Growth factor	1.7	1.2	1.5	1.5	1.5
Fibronectin 1	*Fn1*	25661	Integrin signaling	ECM	1.4	1.3	1.5	1.6	1.5
A kinase (PRKA) anchor protein (gravin) 12	*Akap12*	83425	Scaffolding protein	Signal transduction	1.2	1.6	1.6	1.3	1.4
Neuronatin	*Nnat*	94270	Protein transport		2.0	1.4	1.5	0.9	1.4
Glycosylation dependent cell adhesion molecule 1	*Glycam1*	25258	Selectin ligand	Differentiation	0.5	2.2	1.2	1.7	1.4
Secreted acidic cysteine rich glycoprotein	*Sparc*	24791	ECM Formation	ECM	1.6	1.1	1.4	1.4	1.4
Ectonucleotide pyrophosphatase/ phosphodiesterase 2	*Enpp2*	84050	Lysophospholipase	Cell motility	2.1	1.4	1.4	1.0	1.4
Lectin, galactose binding, soluble 1	*Lgals1*	56646	Integrin signaling	ECM	1.5	1.2	1.4	1.4	1.4
Inhibitor of DNA binding 1, helix-loop-helix protein	*Id1*	25261	Transcriptional repression	Tgf-β	1.4	1.4	1.4	1.1	1.4
Follistatin-like 1	*Fstl1*	79210			1.5	1.7	1.2	1.2	1.4
Phosphoserine aminotransferase 1	*Psat1*	293820	Serine biosynthesis	Metabolism	1.4	1.2	1.5	1.3	1.4
Lumican	*Lum*	81682	Proteoglycan	ECM	1.3	1.5	1.1	1.4	1.3
Melanocyte-specific gene 1 protein	*Cited1*	64466	Transcription factor	Signal transduction	1.4	1.9	1.2	1.3	1.3
Serine proteinase inhibitor, clade H, member 1	*Serpinh1*	29345	Procollagen binding	ECM	1.4	1.3	1.3	1.4	1.3
Sushi-repeat-containing protein	*Sprx*	64316			1.3	1.3	1.3	1.5	1.3
Carboxylesterase 3	*Ces3*	113902	Fatty acid metabolism	Metabolism	1.8	1.1	1.3	1.4	1.3
Cysteine rich protein 61	*Cyr61*	83476	Integrin signaling	ECM	1.1	1.3	1.3	1.6	1.3
Solute carrier family 1, member 3	*Slc1a3*	29483	Amino acid transporter	Transporter	1.4	1.3	1.3	1.1	1.3
Similar to RIKEN cDNA 6330406I15	*RDG1307396*	360757			1.6	1.2	1.3	1.3	1.3
Catalase	*Cat*	24248	Hydrogen peroxide reductase	ROS	1.7	1.0	1.4	1.2	1.3
Tropomyosin 1, α	*Tpm1*	24851	Actin binding		1.1	1.3	1.3	1.3	1.3
Activity and neurotransmitter-induced early gene protein 4	*Ania4*	360341	CAM kinase	Kinase	1.5	1.2	1.2	1.3	1.3
Solute carrier family 11, member 2	*Slc11a2*	25715	Divalent metal ion transporter	Transporter	1.4	1.0	1.3	1.2	1.3
Inhibitor of DNA binding 3, helix-loop-helix protein	*Id3*	25585	Transcriptional repression	Tgf-β	1.5	1.2	1.3	0.9	1.3
Solute carrier family 25 member 4	*Slc25a4*	85333	Nucleotide translocator	Transporter	1.3	1.3	1.2	1.3	1.3
Growth hormone receptor	*Ghr*	25235	Growth hormone signaling	Growth factor	2.1	1.1	1.2	1.3	1.3
Phosphoglycerate kinase 1	*Pgk1*	24644	Phosphoprotein glycolysis	Metabolism	1.6	1.2	1.3	1.2	1.3

(*Continued on the following page*)

Table 2. Genes down-regulated in parous rats (Cont'd)

Gene name	Symbol	Gene ID	Function	Category	Fold-change G1P1 versus G0P0				
					Lewis	WF	F344	Cop	Median
Cytosolic cysteine dioxygenase 1	*Cdo1*	81718	Cysteine metabolism	Metabolism	1.5	1.2	1.2	1.3	1.3
Mast cell protease 1	*Mcpt1*	29265	Proteolysis	ECM	1.6	1.3	1.2	1.2	1.2
Collagen, type V, α2	*Col5a2*	85250	ECM structural protein	ECM	1.0	1.2	1.3	1.5	1.2
Carbonic anhydrase 3	*Ca3*	54232	Carbon metabolism	Metabolism	1.8	1.2	1.1	1.3	1.2
Tubulin, α1	*Tuba1*	64158	Microtubule component	Cell structure	1.5	1.2	1.2	1.2	1.2
Angiotensin II receptor, type 1	*Agtr1A*	24180	Angiotensin receptor	Signal transduction	1.3	1.2	1.2	1.3	1.2
Collagen, type 1, α 1	*Col1a1*	29393	ECM structural protein	ECM	1.1	1.2	1.2	1.8	1.2
Annexin A5	*Anxa5*	25673	Calcium ion binding		1.6	1.2	1.2	1.2	1.2
Thymosin, β10	*Tmsb10*	50665	Actin binding		1.3	1.2	1.2	1.0	1.2
Tubulin, β5	*Tubb5*	29214	Microtubule component	Cell structure	1.1	1.3	1.2	1.2	1.2
Histone deacetylase 2	*Hdac2*	84577	Chromatin rearrangement		1.2	1.2	1.3	1.1	1.2
Lectin, galactose binding, soluble 7	*Lgals7*	29518	Galactose binding		1.1	1.8	1.2	1.2	1.2
CD74 antigen	*Cd74*	25599		Immune	1.2	1.2	1.0	1.3	1.2
Proteasome 26S subunit, ATPase 2	*Psmc2*	25581	Protein degradation		1.3	1.1	1.2	1.1	1.2
MORF-related gene X	*Morf412*	317413			1.4	1.2	1.1	1.2	1.2

NOTE: Genes identified as down-regulated by at least 1.2-fold in three out of four rat strains as a result of parity are reported from the highest to lowest median fold change. Gene names and symbols are reported based on the Rat Genome Database, and Gene ID according to Entrez Gene. Gene functions and categories are based on Gene Ontology.
Abbreviations: WF, Wistar-Furth; F344, Fischer 344; Cop, Copenhagen.

analysis of independent parous and nulliparous Lewis rat samples (Fig. 4*A*).

Also consistent with our prior observations, parity resulted in a persistent increase in the expression of genes involved in mammary differentiation, including the milk proteins β-casein and γ-casein, and the metal ion transporters ceruloplasmin and tranferrin (ref. 6; Table 1; Fig. 4*A*).

As we have previously shown in the mouse, the 70-gene rat parity-related gene expression signature reflected the increased presence of immune cells in the parous mammary gland. In particular, increased expression of multiple immunoglobulin heavy and light chain genes in the parous gland suggested an increase in the population of plasma cells, whereas up-regulation of *Mmp12* and *Tnfrsf21* was consistent with increased numbers of macrophages and T cells (Table 1; Fig. 4*A*). Similarly, increased antibacterial and antiviral activity was suggested by the up-regulation of *Lbp, Lcn2*, and *Ccl5* (refs. 24–26; Table 1).

Parity results in down-regulation of amphiregulin and the growth hormone/Igf-I axis. Previous gene expression profiling of mouse mammary development revealed that parity results in a persistent decrease in the expression of several growth factor–encoding genes, including *Areg* and *Igf-I* (6). The present study confirmed that decreased expression of *Areg* and *Igf-I* are consistent features of the parous state in rats (Table 2; Fig. 4*B*). Additional evidence supporting parity-induced down-regulation of the growth hormone/Igf-I axis in the mammary glands of multiple rat strains was suggested by a decrease in growth hormone receptor (*Ghr*) expression (Table 2; Fig. 4*B*) as well as an increase in *Igfbp5* expression (Table 1; Fig. 4*A*), which functions to sequester local Igf-I in the ECM (27).

Parity regulates ECM gene expression. Mammary epithelial-ECM interactions play an important role in both normal mammary gland development and tumorigenesis (28). Moreover, persistent changes in the structure and function of the ECM have been shown in the mammary glands of parous rats (29). In the present study, microarray expression profiling suggested that a principal effect of parity in the rodent mammary gland is alteration of ECM gene expression. Thirteen of the 70 genes constituting the parity signature encode ECM structural components or proteins that regulate ECM formation or signaling (Tables 1 and 2). Notably, the majority of ECM-related gene expression changes induced by parity represented decreases in expression, including the ECM structural components, fibronectin 1, lumican, and collagen type I and collagen type V (Table 2). Parity-induced decreases in the expression of genes that regulate ECM formation or cellular interactions were also observed, including, *Sparc, Lgals1, Lgals7, Serpinh1, Cyr61*, and *Mcpt1* (Table 2; Fig. 4*B*).

To determine whether these parity-induced ECM-related gene expression changes were accompanied by differences in ECM structure, we stained histologic sections with Mason's trichrome to evaluate total collagen content. Although proximal epithelial structures seemed similar with respect to periductal trichrome staining (data not shown), a significant decrease in the extent of trichrome staining surrounding distal ducts was observed in the parous gland (Fig. 4*C*). These results provide further evidence that parity results in structural changes in the ECM.

Discussion

Women who have their first child early in life have a substantially reduced lifetime risk of breast cancer, an effect that is largely restricted to ER-positive tumors. Similar to humans, rats frequently develop ER-positive breast cancers and exhibit parity-induced protection against mammary tumorigenesis. In the current study, we set out to identify persistent parity-induced changes in gene expression that are conserved among multiple rat strains that exhibit hormone-induced protection against mammary tumorigenesis. We found that four genetically diverse inbred rat strains exhibit hormone-induced protection against mammary tumorigenesis and share a 70-gene pregnancy-induced expression signature. Our findings constitute the first global survey of parity-induced changes in gene expression in the rat—which represents the principal model for studying this phenomenon—as well as the first study to show conservation of parity-induced gene expression changes in multiple inbred rat strains that exhibit hormone-induced protection. Beyond suggesting that parity-induced protection is as robust and widely conserved a phenomenon in rats as it is in humans, our findings provide new insights into potential mechanisms by which early first-full term pregnancy decreases breast cancer risk.

These current studies extend our previous observations that parity results in persistently increased mammary expression of *Tgfb3* to include multiple additional strains of rats. Notably, loss of Tgf-β signaling in stromal fibroblasts promotes the growth and invasion of mammary carcinomas (30). Tgf-β may also have direct effects on mammary epithelial cells, resulting in the inhibition of mammary tumorigenesis (31). The sum of these effects is predicted to decrease the susceptibility of the parous gland to oncogenic transformation.

One of the most consistent and robust parity-induced changes in gene expression that we have observed in the rodent mammary gland is down-regulation of the epidermal growth factor receptor ligand, *Areg*. AREG is overexpressed in a high proportion of human breast cancers and correlates with large tumor size and nodal involvement (32). Studies in genetically engineered mice and mammary epithelial cell lines suggest an important role for AREG in driving mammary epithelial proliferation, whereas recent evidence indicates that this growth factor may alter the ECM by the regulation of protease expression and secretion, including matrix metalloproteinase-2, matrix metalloproteinase-9, urokinase-type plasminogen activator, and plasminogen activator inhibitor-1 (33). Thus, parity-mediated down-regulation of *Areg* may not only inhibit epithelial proliferation, but may also hinder the invasive abilities of transformed cells in the mammary gland.

In addition to the down-regulation of *Areg*, we have confirmed that parity also results in the persistent down-regulation of *Igf-I*. Notably, a strong positive correlation exists between serum IGF-I levels and breast cancer risk in premenopausal women (34). Local and serum levels of IGF-I are regulated by growth hormone through its interaction with growth hormone receptor (35). Additional findings indicate that parity results in a persistent decrease in circulating growth hormone levels in rats (7); moreover, treatment of parous rats with Igf-I results in an increase in carcinogen-induced mammary tumorigenesis to levels similar to those observed in nulliparous controls (36). Consistent with this, spontaneous dwarf rats, which lack functional growth hormone, are highly resistant to carcinogen-induced mammary tumorigenesis (37).

Additional evidence for down-regulation of the growth hormone/Igf-I axis within the parous mammary gland was suggested in the present study by increases in *Igfbp5* expression and decreases in *Ghr* expression. As such, our findings suggest that—in addition to reducing circulating levels of growth hormone—parity may modulate local expression and activity of Igf-I within the mammary gland. Whereas Igf-I acts directly on mammary epithelial cells to promote proliferation and inhibit apoptosis (38), Igf-I in the mammary gland is likely produced in the stromal compartment in response to Ghr signaling (39). Local regulation of Igf-I activity also occurs through interactions with Igf-I binding proteins, such as Igfbp5, which binds and sequesters Igf-I in the ECM (40). As such, parity-induced down-regulation of Ghr and Igf-I expression in the mammary gland, coupled with up-regulation of Igfbp5 expression, would be predicted to result in decreased Igf-I activity. This represents a

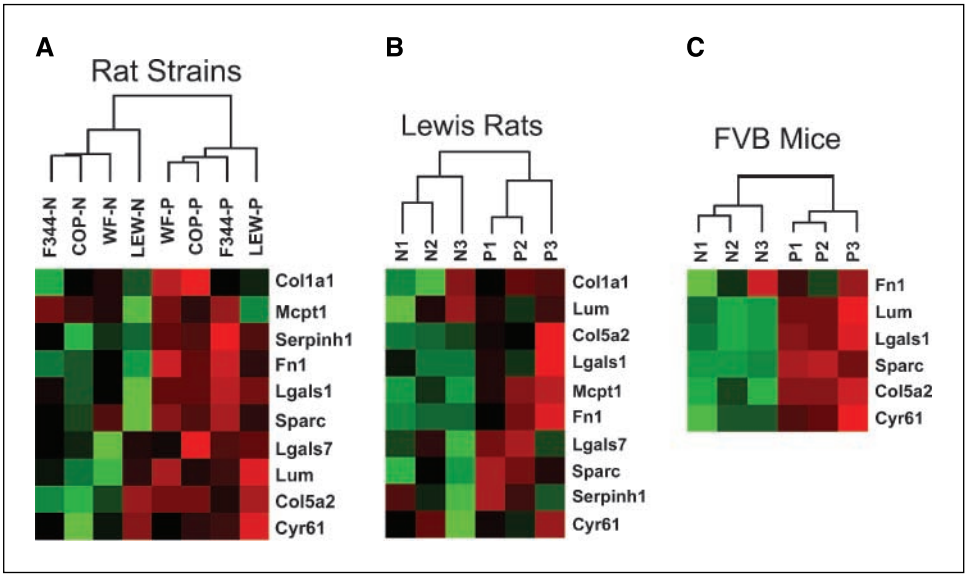

Figure 3. ECM gene expression distinguishes between nulliparous and parous rats and mice. Unsupervised hierarchical clustering analysis. *A,* a subset of parity-regulated genes involved in ECM structure and regulation was used to cluster nulliparous and parous mammary samples from Lewis (*LEW*), Wistar-Furth (*WF*), Fischer (*F344*), and Copenhagen (*COP*) rats. *B,* six independent Lewis samples [three nulliparous (N1-N3) and three parous (P1-P3) samples] were clustered based on the expression of ECM-related genes. *C,* six FVB mouse samples [three nulliparous (N1-N3) and three parous (P1-P3)] were clustered based on the expression of ECM-related genes identified in the rat parity signature that were mapped to the mouse genome.

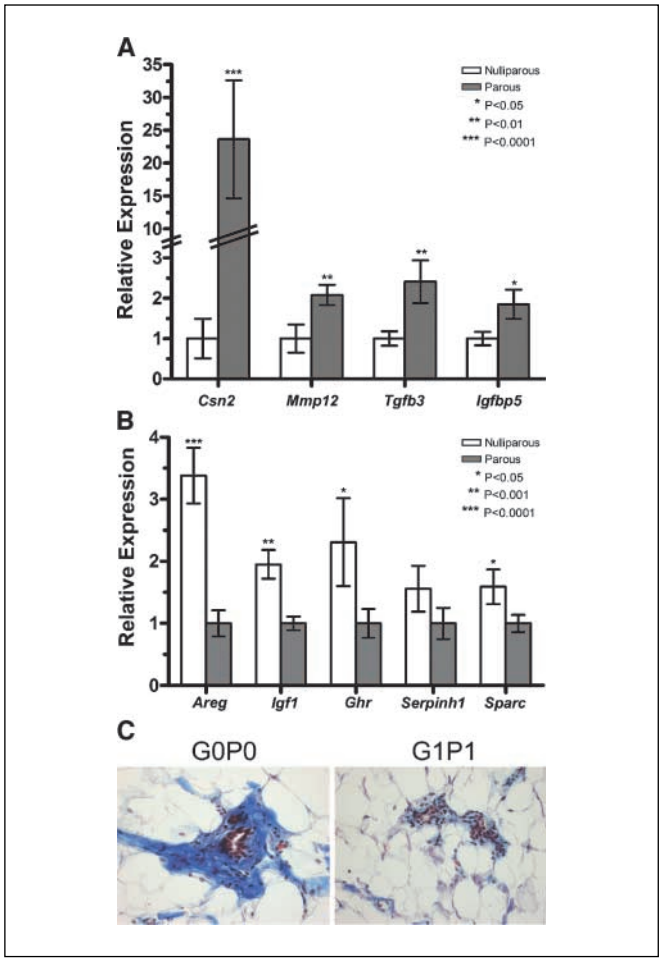

Figure 4. Confirmation of gene expression changes. *A* and *B,* TaqMan QRT-PCR was performed on cDNAs generated from 21 nulliparous and 21 parous Lewis rat mammary samples. Each reaction was performed in duplicate. Expression values for each gene were normalized to *B2m*. *A,* relative expression of parity up-regulated genes. *White columns*, mean expression in nulliparous samples normalized to 1.0 for each gene; *gray columns*, mean expression of each gene in parous relative to nulliparous samples; *bars*, ±SE. *B,* relative expression of parity down-regulated genes. *White columns*, mean expression of each gene in nulliparous relative to parous samples; *gray columns,* mean expression in parous samples normalized to 1.0 for each gene; *bars*, ±SE. *P* values were generated using a one-tailed, unpaired Student's *t* test. *C,* Mason's trichrome staining. Abdominal mammary glands from nulliparous and parous Lewis rats were stained with Mason's trichrome to assess total collagen present in the ECM surrounding epithelial structures. Images are representative of distal structures in the mammary glands of three nulliparous and three parous Lewis rats (original magnification, ×200).

plausible mechanism by which parity may confer protection against breast cancer.

The functional unit of the mammary gland consists of a complex stroma that surrounds the epithelial compartment. Stromal-epithelial interactions play a prominent role, not only in mammary development, but also in tumorigenesis (28). Fibroblasts represent the most prominent cell type of the periductal stroma and, in addition to secreting growth factors that activate epithelial receptors, they are the primary synthesizers of ECM constituents such as fibronectin, collagen, and proteoglycans. Accumulating evidence indicates that stromal constituents, including fibroblasts and ECM structural components, could have differential effects on epithelial cells depending on the source of the tissue from which they are isolated (41). Consistent with this, Schedin et al. have shown that the ability of mammary epithelial cells to form ductal structures in culture is markedly influenced by the developmental context of the ECM in which they are cultured (29). Further support for the role of ECM regulation in parity-induced protection against breast cancer comes from our observation that parous mammary glands exhibit decreased trichrome staining as well as persistent down-regulation of ECM structural and regulatory genes. Because cross-talk between epithelial and stroma cells occurs through local growth factors and their receptors (42), it is possible that parity-induced down-regulation of *Areg* and *Igf-I* in combination with up-regulation of *Tgfb3* may alter stromal-epithelial interactions in such a way as to decrease susceptibility to mammary carcinogenesis.

Finally, it is interesting to speculate that parity-induced changes in the ECM may be related to measures of breast cancer risk associated with mammographic breast density. Increased mammographic density has been consistently shown to correlate with high breast cancer risk (43). Mammographic density has also been reported to be negatively correlated with parity (44). Although breast density was initially believed to reflect the epithelial content of the breast, current evidence suggests that ECM composition—in particular collagen and proteoglycans such as lumican—may be the primary determinant of mammographic density (44, 45). Intriguingly, recent studies have implicated the ratio of serum IGF-I to IGFBP3 as a major determinant of mammographic density (46). Consistent with this, Guo et al. found increased IGF-I tissue staining in samples from women with increased breast density (45). Our findings support the hypothesis that parity decreases Igf-I expression and activity and diminishes the expression of selected ECM structural components. Together, these changes may lead to decreases in both mammographic breast density and breast cancer risk. Validation of this hypothesis will require confirmation that parity alters local IGF-I levels and mammographic breast density in women, and that modulation of Igf-I in rodent models will alter breast density as well as pregnancy-induced protection against breast cancer.

In summary, the results presented in this study extend previous observations that parity results in local changes in growth factor gene expression in the mammary gland. We hypothesize that the evolutionarily conserved parity-induced alterations in gene expression identified in this study result in the modification of the extracellular environment and changes in stromal-epithelial interactions. We hypothesize that the ultimate effect of these changes is to create a tumor suppressive state, thereby providing a potential mechanism to explain parity-induced protection against mammary tumorigenesis. Whether analogous parity-induced changes occur in the human breast remains an important yet unresolved question.

Acknowledgments

Received 11/29/2005; revised 3/28/2006; accepted 4/24/2006.

Grant support: CA92910 from the National Cancer Institute, grants W81XWH-05-1-0405, W81XWH-05-1-0390, DAMD17-03-1-0345 (C.M. Blakely), and DAMD17-00-1-0401 (S.E. Moody) from the U.S. Army Breast Cancer Research Program, and grants from the Breast Cancer Research Foundation and the Emerald Foundation.

The costs of publication of this article were defrayed in part by the payment of page charges. This article must therefore be hereby marked *advertisement* in accordance with 18 U.S.C. Section 1734 solely to indicate this fact.

The authors thank the members of the Chodosh Laboratory for helpful discussions and critical reading of the manuscript.

References

1. Chodosh LA, D'Cruz CM, Gardner HP, et al. Mammary gland development, reproductive history, and breast cancer risk. Cancer Res 1999;59:1765–71.
2. MacMahon B, Cole P, Lin TM, et al. Age at first birth and breast cancer risk. Bull World Health Organ 1970;43: 209–21.
3. Layde PM, Webster LA, Baughman AL, Wingo PA, Rubin GL, Ory HW. The independent associations of parity, age at first full term pregnancy, and duration of breastfeeding with the risk of breast cancer. Cancer and Steroid Hormone Study Group. J Clin Epidemiol 1989;42: 963–73.
4. Russo J, Moral R, Balogh GA, Mailo D, Russo IH. The protective role of pregnancy in breast cancer. Breast Cancer Res 2005;7:131–42.
5. Sivaraman L, Medina D. Hormone-induced protection against breast cancer. J Mammary Gland Biol Neoplasia 2002;7:77–92.
6. D'Cruz CM, Moody SE, Master SR, et al. Persistent parity-induced changes in growth factors, TGF-β3, and differentiation in the rodent mammary gland. Mol Endocrinol 2002;16:2034–51.
7. Thordarson G, Jin E, Guzman RC, Swanson SM, Nandi S, Talamantes F. Refractoriness to mammary tumorigenesis in parous rats: is it caused by persistent changes in the hormonal environment or permanent biochemical alterations in the mammary epithelia? Carcinogenesis 1995;16:2847–53.
8. Russo J, Gusterson BA, Rogers AE, Russo IH, Wellings SR, van Zwieten MJ. Comparative study of human and rat mammary tumorigenesis. Lab Invest 1990;62:244–78.
9. Sivaraman L, Stephens LC, Markaverich BM, et al. Hormone-induced refractoriness to mammary carcinogenesis in Wistar-Furth rats. Carcinogenesis 1998;19: 1573–81.
10. Yang J, Yoshizawa K, Nandi S, Tsubura A. Protective effects of pregnancy and lactation against *N*-methyl-*N*-nitrosourea-induced mammary carcinomas in female Lewis rats. Carcinogenesis 1999;20:623–8.
11. Rajkumar L, Guzman RC, Yang J, Thordarson G, Talamantes F, Nandi S. Short-term exposure to pregnancy levels of estrogen prevents mammary carcinogenesis. Proc Natl Acad Sci U S A 2001;98:11755–9.
12. Guzman RC, Yang J, Rajkumar L, Thordarson G, Chen X, Nandi S. Hormonal prevention of breast cancer: mimicking the protective effect of pregnancy. Proc Natl Acad Sci U S A 1999;96:2520–5.
13. Medina D, Smith GH. Chemical carcinogen-induced tumorigenesis in parous, involuted mouse mammary glands. J Natl Cancer Inst 1999;91:967–69.
14. Medina D, Kittrell FS. p53 function is required for hormone-mediated protection of mouse mammary tumorigenesis. Cancer Res 2003;63:6140–3.
15. Ginger MR, Gonzalez-Rimbau MF, Gay JP, Rosen JM. Persistent changes in gene expression induced by estrogen and progesterone in the rat mammary gland. Mol Endocrinol 2001;15:1993–2009.
16. Colditz GA, Rosner BA, Chen WY, Holmes MD, Hankinson SE. Risk factors for breast cancer according to estrogen and progesterone receptor status. J Natl Cancer Inst 2004;96:218–28.
17. Turcot-Lemay L, Kelly PA. Response to ovariectomy of *N*-methyl-*N*-nitrosourea-induced mammary tumors in the rat. J Natl Cancer Inst 1981;66:97–102.
18. Master SR, Stoddard AJ, Bailey LC, Pan TC, Dugan KD, Chodosh LA. Genomic analysis of early murine mammary gland development using novel probe-level algorithms. Genome Biol 2005;6:R20.
19. Gentleman RC, Carey VJ, Bates DM, et al. Bioconductor: open software development for computational biology and bioinformatics. Genome Biol 2004;5:R80.
20. Phang TL, Neville MC, Rudolph M, Hunter L. Trajectory clustering: a non-parametric method for grouping gene expression time courses, with applications to mammary development. Pac Symp Biocomput 2003;351–62.
21. Waha A, Sturne C, Kessler A, et al. Expression of the ATM gene is significantly reduced in sporadic breast carcinomas. Int J Cancer 1998;78:306–9.
22. Ito K, Fujimori M, Nakata S, et al. Clinical significance of the increased multidrug resistance-associated protein (MRP) gene expression in patients with primary breast cancer. Oncol Res 1998;10:99–109.
23. Gould MN, Zhang R. Genetic regulation of mammary carcinogenesis in the rat by susceptibility and suppressor genes. Environ Health Perspect 1991;93:161–7.
24. Flo TH, Smith KD, Sato S, et al. Lipocalin 2 mediates an innate immune response to bacterial infection by sequestrating iron. Nature 2004;432:917–21.
25. Elliott MB, Tebbey PW, Pryharski KS, Scheuer CA, Laughlin TS, Hancock GE. Inhibition of respiratory syncytial virus infection with the CC chemokine RANTES (CCL5). J Med Virol 2004;73:300–8.
26. Branger J, Florquin S, Knapp S, et al. LPS-binding protein-deficient mice have an impaired defense against Gram-negative but not Gram-positive pneumonia. Int Immunol 2004;16:1605–11.
27. Flint DJ, Beattie J, Allan GJ. Modulation of the actions of IGFs by IGFBP-5 in the mammary gland. Horm Metab Res 2003;35:809–15.
28. Tlsty TD, Hein PW. Know thy neighbor: stromal cells can contribute oncogenic signals. Curr Opin Genet Dev 2001;11:54–9.
29. Schedin P, Mitrenga T, McDaniel S, Kaeck M. Mammary ECM composition and function are altered by reproductive state. Mol Carcinog 2004;41:207–20.
30. Cheng N, Bhowmick NA, Chytil A, et al. Loss of TGF-β type II receptor in fibroblasts promotes mammary carcinoma growth and invasion through upregulation of TGF-α-, MSP- and HGF-mediated signaling networks. Oncogene 2005;24:5053–68.
31. Pierce DF, Jr., Gorska AE, Chytil A, et al. Mammary tumor suppression by transforming growth factor β1 transgene expression. Proc Natl Acad Sci U S A 1995;92: 4254–8.
32. Ma L, de Roquancourt A, Bertheau P, et al. Expression of amphiregulin and epidermal growth factor receptor in human breast cancer: analysis of autocriny and stromal-epithelial interactions. J Pathol 2001;194:413–9.
33. Menashi S, Serova M, Ma L, Vignot S, Mourah S, Calvo F. Regulation of extracellular matrix metalloproteinase inducer and matrix metalloproteinase expression by amphiregulin in transformed human breast epithelial cells. Cancer Res 2003;63:7575–80.
34. Schernhammer ES, Holly JM, Pollak MN, Hankinson SE. Circulating levels of insulin-like growth factors, their binding proteins, and breast cancer risk. Cancer Epidemiol Biomarkers Prev 2005;14:699–704.
35. Laban C, Bustin SA, Jenkins PJ. The GH-IGF-I axis and breast cancer. Trends Endocrinol Metab 2003;14:28–34.
36. Thordarson G, Slusher N, Leong H, et al. Insulin-like growth factor (IGF)-I obliterates the pregnancy-associated protection against mammary carcinogenesis in rats: evidence that IGF-I enhances cancer progression through estrogen receptor-α activation via the mitogen-activated protein kinase pathway. Breast Cancer Res 2004;6:R423–36.
37. Thordarson G, Semaan S, Low C, et al. Mammary tumorigenesis in growth hormone deficient spontaneous dwarf rats; effects of hormonal treatments. Breast Cancer Res Treat 2004;87:277–90.
38. Hadsell DL, Bonnette SG. IGF and insulin action in the mammary gland: lessons from transgenic and knockout models. J Mammary Gland Biol Neoplasia 2000;5:19–30.
39. Gallego MI, Binart N, Robinson GW, et al. Prolactin, growth hormone, and epidermal growth factor activate Stat5 in different compartments of mammary tissue and exert different and overlapping developmental effects. Dev Biol 2001;229:163–75.
40. Marshman E, Green KA, Flint DJ, White A, Streuli CH, Westwood M. Insulin-like growth factor binding protein 5 and apoptosis in mammary epithelial cells. J Cell Sci 2003;116:675–82.
41. Barcellos-Hoff MH, Ravani SA. Irradiated mammary gland stroma promotes the expression of tumorigenic potential by unirradiated epithelial cells. Cancer Res 2000;60:1254–60.
42. Bhowmick NA, Neilson EG, Moses HL. Stromal fibroblasts in cancer initiation and progression. Nature 2004;432:332–7.
43. Tice JA, Cummings SR, Ziv E, Kerlikowske K. Mammographic breast density and the Gail model for breast cancer risk prediction in a screening population. Breast Cancer Res Treat 2005;94:115–22.
44. Li T, Sun L, Miller N, et al. The association of measured breast tissue characteristics with mammographic density and other risk factors for breast cancer. Cancer Epidemiol Biomarkers Prev 2005;14:343–9.
45. Guo YP, Martin LJ, Hanna W, et al. Growth factors and stromal matrix proteins associated with mammographic densities. Cancer Epidemiol Biomarkers Prev 2001;10:243–8.
46. Diorio C, Pollak M, Byrne C, et al. Insulin-like growth factor-I, IGF-binding protein-3, and mammographic breast density. Cancer Epidemiol Biomarkers Prev 2005;14:1065–73.

Research article

Open Access

Dense breast stromal tissue shows greatly increased concentration of breast epithelium but no increase in its proliferative activity

Debra Hawes[1], Susan Downey[2], Celeste Leigh Pearce[3], Sue Bartow[4], Peggy Wan[3], Malcolm C Pike[3] and Anna H Wu[3]

[1]Department of Pathology, Keck School of Medicine, University of Southern California, 2011 Zonal Avenue, Los Angeles, CA 90089, USA
[2]Department of Surgery, Keck School of Medicine, University of Southern California, 1510 San Pablo Street, Los Angeles, CA 90033, USA
[3]Department of Preventive Medicine, Keck School of Medicine, University of Southern California/Norris Comprehensive Cancer Center, 1441 Eastlake Avenue, Los Angeles, CA 90033, USA
[4]107 Stark Mesa, Carbondale, CO 81623, USA

Corresponding author: Malcolm C Pike, mcpike@usc.edu

Received: 2 Feb 2006 Revisions requested: 21 Feb 2006 Revisions received: 8 Mar 2006 Accepted: 30 Mar 2006 Published: 28 Apr 2006

Breast Cancer Research 2006, **8**:R24 (doi:10.1186/bcr1408)
This article is online at: http://breast-cancer-research.com/content/8/2/R24

Abstract

Introduction Increased mammographic density is a strong risk factor for breast cancer. The reasons for this are not clear; two obvious possibilities are increased epithelial cell proliferation in mammographically dense areas and increased breast epithelium in women with mammographically dense breasts. We addressed this question by studying the number of epithelial cells in terminal duct lobular units (TDLUs) and in ducts, and their proliferation rates, as they related to local breast densities defined histologically within individual women.

Method We studied deep breast tissue away from subcutaneous fat obtained from 12 healthy women undergoing reduction mammoplasty. A slide from each specimen was stained with the cell-proliferation marker MIB1. Each slide was divided into (sets of) areas of low, medium and high density of connective tissue (CT; highly correlated with mammographic densities). Within each of the areas, the numbers of epithelial cells in TDLUs and ducts, and the numbers MIB1 positive, were counted.

Results The relative concentration (RC) of epithelial cells in high compared with low CT density areas was 12.3 (95% confidence interval (CI) 10.9 to 13.8) in TDLUs and 34.1 (95% CI 26.9 to 43.2) in ducts. There was a much smaller difference between medium and low CT density areas: RC = 1.4 (95% CI 1.2 to 1.6) in TDLUs and 1.9 (95% CI 1.5 to 2.3) in ducts. The relative mitotic rate (RMR; MIB1 positive) of epithelial cells in high compared with low CT density areas was 0.59 (95% CI 0.53 to 0.66) in TDLUs and 0.65 (95% CI 0.53 to 0.79) in ducts; the figures for the comparison of medium with low CT density areas were 0.58 (95% CI 0.48 to 0.70) in TDLUs and 0.66 (95% CI 0.44 to 0.97) in ducts.

Conclusion Breast epithelial cells are overwhelmingly concentrated in high CT density areas. Their proliferation rate in areas of high and medium CT density is lower than that in low CT density areas. The increased breast cancer risk associated with increased mammographic densities may simply be a reflection of increased epithelial cell numbers. Why epithelium is concentrated in high CT density areas remains to be explained.

Introduction

On a mammogram, fat appears radiolucent or dark, whereas stromal and epithelial tissue appears radio-dense or white. The amount of mammographic density is a strong independent predictor of breast cancer risk [1,2]. The biological basis for this increased risk is poorly understood. A critical question is whether densities are directly related to risk or are simply a marker of risk. We addressed this question recently by studying the location of small ductal carcinoma *in situ* (DCIS) lesions as revealed by microcalcifications, and showed that such DCIS occurs overwhelmingly in the mammographically dense areas of the breast [3]. Most DCIS lesions in our study

a_H, a_L, a_M = the areas of the slide classified as being of high, low and medium CT density (in μm^2); CI = confidence interval; CT = connective tissue; DAB = 3,3'-diaminobenzidine tetrahydrochloride; DCIS = ductal carcinoma *in situ*; n_H, n_L, n_M = the numbers of epithelial cells staining positive for MIB1 within high, low and medium CT density areas; RC = relative concentration; RMR = relative mitotic rate; TDLU = terminal duct lobular unit; t_H, t_L, t_M = the numbers of epithelial cells within high, low and medium CT density areas;

Table 1

Relation between relative concentration of epithelial cells and connective tissue density

CT density	RC	95% CI	*p*
TDLUs			
Low	1.0		
Medium	1.4	1.2–1.6	<0.001
High	12.3	10.9–13.8	<0.001
Ducts			
Low	1.0		
Medium	1.9	1.5–2.3	<0.001
High	34.1	26.9–43.2	<0.001

CI, confidence interval; CT, connective tissue; RC, relative concentration (per unit area); TDLUs, terminal duct lobular units.

occurred in the lateral-superior quadrant, as has been found in previous studies [4], and 'correlated strongly with the average percentage density in the different mammographic quadrants' [3]. Pre-DCIS mammograms that were taken on average about two years previously showed that the areas subsequently exhibiting DCIS were clearly dense at the time of the earlier mammogram, and this suggests that this relationship was not brought about by the presence of the DCIS. The reasons for these findings are not clear; two obvious possibilities are increased epithelial cell proliferation in mammographically dense areas of the breast and increased breast epithelium in women with mammographically dense breasts. Two groups have investigated the relationship between the amount of mammographic density of a woman and the amount of her breast epithelial tissue [5,6]. Alowami and colleagues [5] used tissue obtained from biopsies investigating breast lesions that were subsequently diagnosed as benign or pre-invasive breast disease; they studied tissue 'distant from the diagnostic lesion' without reference to its location as regards mammographic density (that is, 'random' tissue). They found that the median density of duct lobular units was 28% higher in breasts whose overall mammographic density was 50% or more ($n = 27$) than in breasts whose overall mammographic density was less than 25% ($n = 35$); this result was not statistically significant and the result was described as showing 'no difference in the density of epithelial components' [5]. Li and colleagues [6] also found in their much larger study ($n = 236$) of 'random' breast tissue collected from normal women by Bartow and colleagues [7] in their autopsy study of accidental deaths in New Mexico that women with high mammographic density had greater amounts of epithelial tissue (as measured by area of epithelial nuclear staining) and the result was highly statistically significant. Breast epithelial proliferation rates as they relate to mammographic densities in healthy women have not been well studied [8]. We have addressed these questions by studying the number of epithelial cells in terminal duct lobular units (TDLUs) and in breast ducts, and their respective proliferation rates as they relate to local histological breast densities within individual women.

Materials and methods

We retrospectively identified 15 consecutive healthy women who had undergone a reduction mammoplasty performed by one of us (SD) at the University of Southern California medical facilities. The study protocol was approved by the Institutional Review Board of the University of Southern California School of Medicine.

For each participant we obtained the formalin-fixed paraffin-embedded block of tissue that had been routinely processed and saved from her surgery. A single slide was cut from each block and stained with the proliferation marker MIB1 (BioGenex Laboratories, San Ramon, CA, USA). The slides were prepared in accordance with our previously published protocol [9]; the chromogen used was 3,3'-diaminobenzidine tetrahydrochloride (DAB). On microscopic examination one of the slides contained skin and two other slides showed areas of disintegration; all three were deemed unsuitable for study.

Each of the remaining 12 slides was divided into (sets of) areas of low, medium and high density of connective tissue (CT) (highly correlated with densities as defined by mammographic criteria [10]); see Figure 1. The total size of each of the three areas (in μm^2), and within each of the three areas the numbers of epithelial cells in TDLUs and ducts and the numbers that were MIB1 positive, were counted with the help of an automated microscope system that digitized the images and permitted the outlining of relevant areas on a high-resolution computer screen (ACIS II; Clarient, Inc., San Juan Capistrano, CA, USA). The total numbers of epithelial cells in different outlined areas within the CT density-defined areas was then automatically counted by the ACIS II nuclear counting software program, which is based on color identification. Hematoxylin was used to counterstain the MIB1-negative nuclei blue, and the DAB chromogen marked the MIB1-positive nuclei brown.

Figure 1

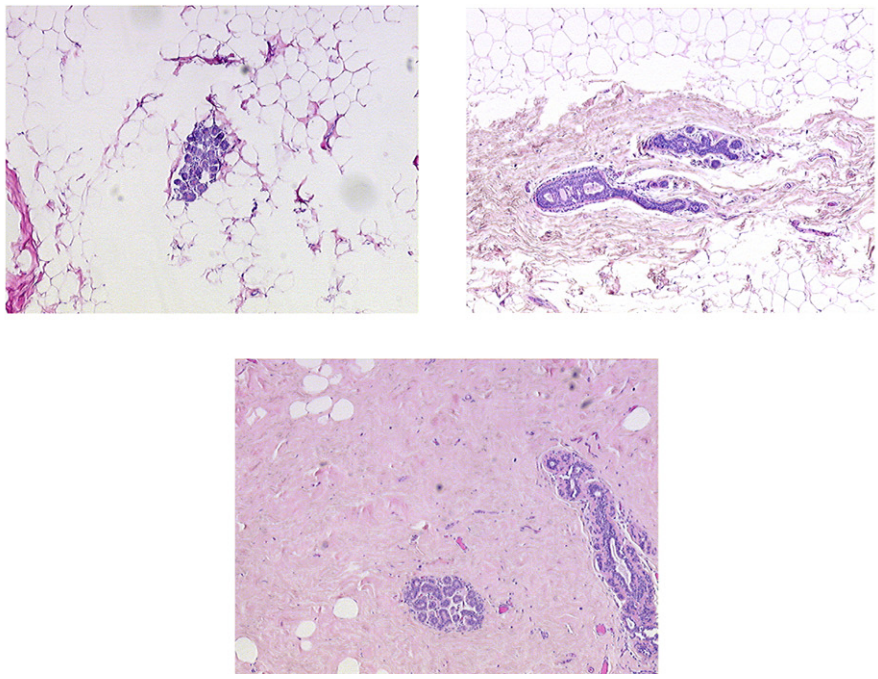

Example of areas of low, medium (upper right) and high (lower center) CT density.

The software calculated the numbers of MIB1-negative and MIB1-positive cells on the basis of these color differences.

Statistical analysis

For each slide, and separately for TDLU and ductal cells, three sets of values were obtained: first, the areas of the slide classified as being of low, medium or high CT density (a_L, a_M and a_H in μm^2); second, the numbers of epithelial cells within these areas (t_L, t_M and t_H); and third, the numbers of these epithelial cells staining positive for MIB1 (n_L, n_M and n_H). On the null hypothesis of no association between the *t*'s and the *a*'s – that is, no association between the numbers of epithelial cells and the CT density of the local tissue – the expected value of the *t*'s is simply proportional to the related *a*'s, so that, for example, the expected value of t_H is $(t_L + t_M + t_H) \times a_H/(a_L + a_M + a_H)$. Similarly, on the null hypothesis of no association between MIB1 positivity as a proportion of epithelial cells and the CT density of the local tissue, the expected value of the *n*'s is simply proportional to the related *t*'s, so that, for example, the expected value of n_H is $(n_L + n_M + n_H) \times t_H/(t_L + t_M + t_H)$. We analyzed these data with standard statistical software as implemented in the STATA statistical software package (procedure cs; Stata Corporation, Austin, TX, USA); the ratios of epithelial concentration (cells per unit area) and the ratios of proportions of epithelial cells staining positive for MIB1 are the measures of effect. All statistical significance levels (*p* values) quoted are two-sided.

Results

The 12 subjects included in the analysis were aged 18 to 60 years with a median age of 33 years; only one subject was aged 50 years or older.

Areas of the slides of low CT density comprised on average 44% of the total of areas of low plus medium plus high CT density ($a_L/(a_L + a_M + a_H)$), whereas areas of high CT density comprised on average 35% of the total area ($a_H/(a_L + a_M + a_H)$).

Table 1 shows the summary relative concentrations (RCs; ratios of cells per unit area) of epithelial cells in the three areas defined by CT density separately for TDLU cells and for ductal cells. The concentration of TDLU epithelial cells is slightly greater in the areas of medium CT density than in the areas of low CT density (RC = 1.4, 95% confidence interval (CI) 1.2 to 1.6; $p < 0.001$) but is much greater in the areas of high CT density (RC = 12.3, 95% CI 10.8 to 13.8; $p < 0.001$). The TDLU results for the individual slides (women) comparing areas of high CT density with areas of low CT density are shown in Figure 2. Although the results from individual subjects do differ somewhat, the RCs were not correlated with age (the only variable available on these women) and the summary RC seems to be a fair representation of the overall results. The results for ducts were similar.

Table 2 shows the summary relative mitotic rates (RMRs) of epithelial cells staining MIB1 positive in the three areas defined by CT density separately for TDLU cells and for ductal

Table 2

Relation between relative mitotic rate (MIB1 positive) of epithelial cells and connective tissue density

CT density	RMR	95% CI	*p*
TDLUs			
Low	1.00		
Medium	0.58	0.48–0.70	<0.001
High	0.59	0.53–0.66	<0.001
Ducts			
Low	1.00		
Medium	0.66	0.44–0.97	0.035
High	0.65	0.53–0.79	<0.001

CI, confidence interval; CT, connective tissue; RMR, relative mitotic rate; TDLUs, terminal duct lobular units.

Figure 2

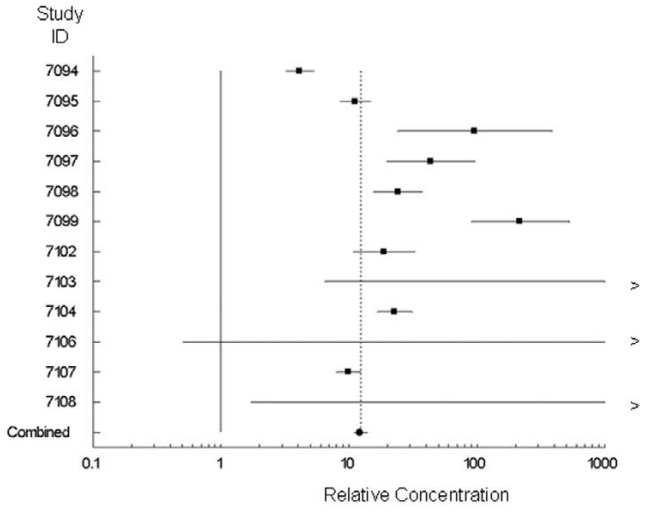

RCs (with 95% CIs) of TDLU epithelial cells in high and low CT areas.

Figure 3

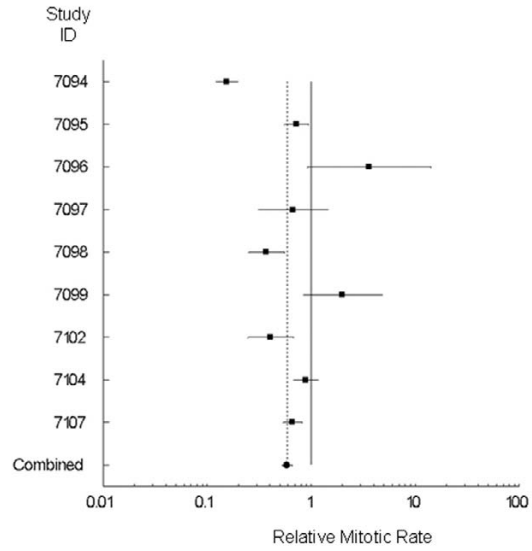

RMRs (with 95% CIs) of TDLU epithelial cells in high and low CT areas.

cells. The proportion of TDLU epithelial cells staining MIB1 positive is statistically significantly less (RMR ≈ 0.6) both in the areas of medium CT density ($p < 0.001$) and in the areas of high CT density ($p < 0.001$) than in the areas of low CT density. The median MIB1-positive proportion was about 4%. Almost all the women in this study were premenopausal on the basis of their age; this figure is close to the Ki67 figure of 4.5% given for healthy premenopausal women in the study of Hargreaves and colleagues [11]. The TDLU results for the individual slides (women) comparing areas of high CT density with areas of low CT density are shown in Figure 3. Again, although the results from individual subjects do differ somewhat, the RMRs were not correlated with age (the only variable available on these women) and the summary RMR seems to be a fair representation of the overall results. The results for ducts were again similar. There was no difference in the proliferation rates of epithelial cells in TDLUs and ducts within the same CT density area of individual women (RMR = 1.01, 95% CI 0.98 to 1.04; $p = 0.42$).

More details of the results are provided in the Additional file.

Discussion

Mammographic density is a very strong risk factor for breast cancer. The two groups of investigators [5,6] that studied random biopsies (single slides) from women with different mammographic densities found that the extent of mammographic densities was most strongly correlated with the amount of collagen on the slide. A weaker correlation was found with the amount of epithelial tissue. The findings reported here suggest that the relation between the extent of mammographic density and the amount of epithelial tissue is directly related to the increased concentration of collagen (the main component of

'connective tissue' as shown by collagen staining; see Figure 1) in women with high mammographic densities, because breast epithelium is overwhelmingly confined to areas of high CT density. In the earlier studies of random biopsies [5,6] the weaker relationship between mammographic density and epithelium concentration than between mammographic density and collagen concentration could be simply due to the much greater statistical variability of epithelial tissue in a random slide than one would see for collagen, which occupies a much greater extent of the slide. These results suggest that the increasing breast cancer risk associated with increasing mammographic density might be simply a reflection of more breast epithelial tissue.

We found that the proliferation rate of epithelial cells in areas of high CT density was much lower than in areas of low CT density, arguing against the possibility that dense stroma has a growth factor role in the increased breast cancer risk of women with mammographically dense breasts. In the study of Stomper and colleagues [8], comparison was made between single biopsies of either fat or dense areas in different women; they found no difference in the proliferation rates in the dense and fat areas. Further work is warranted but there is clearly no evidence that areas of high CT density are associated with increased proliferation.

Our results were obtained by conducting a comprehensive count of all the cells in each slide per subject (instead of counting a selected region) and allowed the comparison of proliferation rates in areas of differing CT density within an individual. This permitted us to control completely automatically for factors such as age, menopausal status, or time in the menstrual cycle in the analysis. This gave us great statistical power so that highly statistically significant results could be obtained even with small numbers of subjects.

This study used tissue obtained at reduction mammoplasty performed on women with large breasts. We do not believe that this affects the validity of our findings because the tissue samples were taken deep in the breast away from the subcutaneous fat, but this requires confirmation in future studies. Further studies are also needed relating the CT densities to such risk factors as parity and to understand the biology of the relationship between CT densities and breast epithelium.

Conclusion

The basis of the strong relationship between mammographic density and breast cancer risk may be simply that mammographically dense breasts contain more breast epithelial tissue. Why breast epithelial tissue should be associated with CT densities is not known. Does breast epithelium induce densities? Alternatively, can breast epithelium effectively survive only in areas of densities? Understanding the nature of the interaction between dense CT stroma and epithelial tissue should be a major focus of breast cancer research.

Competing interests

The authors declare that they have no competing interests.

Authors' contributions

DH, AHW, CLP and MCP participated in the design of the study. DH supervised the preparation of the slides and analyzed the slides with the ACIS II system. SD performed all the reduction mammoplasties that provided the tissues used in this analysis and consulted on the tissue obtained from reduction mammoplasties. SB consulted on the interpretation of the results and provided insight into the relationship between mammographic densities and tissue characteristics. CLP coordinated the study. MCP supervised the statistical analysis which was carried out by PW. AHW, CLP and MCP conceived of the study. MCP, DH and AHW drafted the manuscript; all authors read and approved the final manuscript.

Additional files

The following Additional files are available online:

Additional File 1

A Word file containing two tables of detailed results from this study.
See http://www.biomedcentral.com/content/supplementary/bcr1408-S1.doc

Acknowledgements

This work was supported by a Department of Defense Congressionally Mandated Breast Cancer Program Grant BC 044808, by the USC/Norris Comprehensive Cancer Center Core Grant P30 CA14089, and by generously donated funds from the endowment established by Flora L Thornton for the Chair of Preventive Medicine at the USC/Norris Comprehensive Cancer Center. The funding sources had no role in this report.

References

1. Saftlas AF, Szklo M: **Mammographic parenchymal patterns and breast cancer risk.** *Epidemiol Rev* 1987, **9:**146-174.
2. Boyd NF, Lockwood GA, Byng JW, Tritchler DL, Yaffe MJ: **Mammographic densities and breast cancer risk.** *Cancer Epidemiol Biomarkers Prev* 1998, **7:**1133-1144.
3. Ursin G, Hovanessian-Larsen L, Parisky YR, Pike MC, Wu AH: **Greatly increased occurrence of breast cancers in areas of mammographically dense tissue.** *Breast Cancer Res* 2005, **7:**R605-R608.
4. Perkins CI, Hotes J, Kohler BA, Howe HL: **Association between breast cancer laterality and tumor location, United States, 1994-1998.** *Cancer Causes Control* 2004, **15:**637-645.
5. Alowami S, Troup S, Al-Haddad S, Kirkpatrick I, Watson PH: **Mammographic density is related to stroma and stromal proteoglycan expression.** *Breast Cancer Res* 2003, **5:**R129-R135.
6. Li T, Sun L, Miller N, Nicklee T, Woo J, Hulse-Smith L, Tsao M-S, Khokha L, Martin L, Boyd N: **The association of measured breast tissue characteristics with mammographic density and other risk factors for breast cancer.** *Cancer Epidemiol Biomarkers Prev* 2005, **14:**343-349.
7. Bartow SA, Pathak DR, Black WC, Key CR, Teaf SR: **The prevalence of benign, atypical and malignant breast lesions in pop-**

ulations at different risk for breast cancer. *Cancer* 1987, **60:**2751-2760.
8. Stomper PC, Penetrante RB, Edge SB, Arredondo MA, Blumenson LE, Stewart CC: **Cellular proliferative activity of mammographic normal dense and fatty tissue determined by DNA S phase percentage.** *Breast Cancer Res Treat* 1996, **37:**229-236.
9. Shi S-R, Cote R, Chaiwun B, Young LL, Shi Y, Hawes D, Chen T, Taylor CR: **Standardization of immunochemistry based on antigen retrieval technique for routine formalin-fixed tissue sections.** *Appl Immunohistochem* 1998, **6:**89-96.
10. Bartow SA, Mettler FA, Black WC, Moskowitz M: **Correlations between radiographic patterns and morphology of the female breast.** *Prog Surg Path* 1982, **4:**263-275.
11. Hargreaves DF, Potten CS, Harding C, Shaw LE, Morton MS, Roberts SA, Howell A, Bundred NJ: **Two-week dietary soy supplementation has an estrogenic effect on normal premenopausal breast.** *J Clin Endocrinol Metab* 1999, **84:**4017-4024.

Personnel List

University of Southern California

Malcolm C. Pike
Anna H. Wu
C. Leigh Pearce
Debra Hawes
Michael F. Press
Sue Ellen Martin
Frank Stanczyk
Jonathan Buckley
Lilly Chang
Alex Trana
Angela Umali
Peggy Wan
Lillian Young
Heidi St. Royal
Yongtian Li
Randall Widelitz

University of Pennsylvania

Lewis H. Chodosh
George Belka
Celina D'Cruz
Kate Dugan
Raina Fitzgerald-Anderson
Zhandong Liu
Kathy Notarfrancesco
Tien-chi Pan
Barbara Sheilds
Judith Smith
Alex Stoddard
Patrick Taulman
Jinling Wu